Ecological Modelling 521 (2026) 111763

Contents lists available at ScienceDirect

Ecological Modelling

journal homepage: www.elsevier.com/locate/ecolmodel

Machine learning for modeling forest dynamics using National Forest Inventory and climate data

Dea Rieder [a,*], Maximiliano Costa [b], Christian Temperli [c], Francesco Giardina [d], Giacomo Vaccario [a]

[a] Chair of Ecosystem Management, ETH Zürich, Switzerland
[b] Chair of Forest Ecology, ETH Zürich, Switzerland
[c] Forest Resources and Management, Swiss Federal Institute for Forest, Snow and Landscape Research WSL, Switzerland
[d] Institute of Terrestrial Ecosystems, ETH Zürich, Switzerland

ARTICLE INFO

Keywords:
Forest dynamics
Machine learning
Climate change
National Forest Inventory
Basal area
Species composition

ABSTRACT

Accurate prediction of forest structure and composition is essential for forest management, as planning depends on anticipating future stand dynamics under changing environmental conditions. Machine learning algorithms have proven useful for this task due to their ability to capture non-linear ecological patterns in forest dynamics. However, current machine learning applications in forest ecology mostly focus on component growth rates, leaving approaches that directly predict future stand-level states like total basal area and species composition under-explored. This study develops a national-scale XGBoost model for Swiss forests, using Swiss National Forest Inventory data and CH2018 climate scenarios to predict changes in basal area and broadleaf proportion. Tested on a later inventory not used for training, XGBoost predicts the next inventory state with an R^2 of 0.66 for basal area and 0.91 for broadleaf proportion, slightly above a linear Lasso model (0.65 and 0.90). When applied recursively to generate exploratory projections to 2099, the model indicates an overall increase in basal area, although unmanaged lower-elevation belts decrease, and an increase in broadleaf proportion mainly at lower elevations, especially under high emissions. These trends are similar to patterns reported by established process-based and empirical forest models. This work offers a computationally efficient approach for projecting forest dynamics over large areas, without the extensive parameterization required by process-based models.

1. Introduction

Forests provide many ecosystem functions and services at both global and local scales (Brockerhoff et al., 2017). These services include timber production, habitat provision for native and endangered species, climate regulation by sequestering carbon dioxide, and cultural services (Brockerhoff et al., 2017; Krieger, 2001). However, forest ecosystems are already experiencing impacts from changing temperatures, precipitation patterns, and increased disturbance frequency resulting from climate change (Henne et al., 2018; Seidl et al., 2017). Globally, observed effects include changes in forest growth (Piao et al., 2011), species distribution (Iverson and McKenzie, 2013; Walther, 2003), and mortality induced by drought (Allen et al., 2010; Senf et al., 2018) and other disturbances such as storms, bark beetles and wildfires (Seidl et al., 2017). Such changes have already affected the ecosystem services that forests provide (Elkin et al., 2013; Wolf and Paul-Limoges, 2023). Climate change is expected to have many impacts on forests, affecting their productivity and biomass (Brecka et al., 2018). Tree species are projected to shift to higher elevations and be replaced by more drought- and warm-adapted species at lower altitudes (Peñuelas and Boada, 2003; Walther et al., 2002). In Switzerland, for instance, projections from the process-based model ForClim and the empirical model MASSIMO indicate a basal area increase at higher elevations and a shift toward broadleaf species at lower elevations and in managed forests (Huber et al., 2021; Stadelmann et al., 2019; Flury et al., 2024).

Forest modeling is important for forest management decisions (Rittenhouse et al., 2011; Zollner et al., 2005), as strategic forest management planning requires the ability to predict and evaluate future forest structure and composition (Taylor, 2009). To adapt forest management to a changing climate, it is also necessary to predict how climate change effects will evolve over time (Keenan, 2015). In addition, with regard to international commitments such as the Kyoto Protocol, the European Union proposed that countries provide specific estimates on the present state and future development of their forests' carbon balance (Krug, 2018; Stadelmann et al., 2019). To make these types of estimates and

* Corresponding author.
E-mail address: riederd@ethz.ch (D. Rieder).

https://doi.org/10.1016/j.ecolmodel.2026.111763
Received 5 April 2026; Received in revised form 19 July 2026; Accepted 23 July 2026
Available online 5 August 2026

assist policymakers, many European countries have developed forest projection systems (Barreiro et al., 2016). For example, in Switzerland, the empirical forest development model MASSIMO is used to make predictions at national scale based on forest inventory data (Thürig et al., 2021).

Forest development can be modeled with process-based and empirical approaches (Fontes et al., 2010). Process-based models use mechanistic representations of eco-physiological and demographic processes, including photosynthesis, growth, and mortality, to simulate forest dynamics (Mäkelä et al., 2000). These models capture underlying processes to allow assessments under projected future climate conditions (Gustafson, 2013). Accordingly, these models are commonly applied to project forest dynamics over decades to centuries (Bugmann and Seidl, 2022; Shifley et al., 2017). However, their projections — particularly over short- to intermediate-term horizons relevant for management — can be highly sensitive to how initial forest conditions and parameters are specified (Temperli et al., 2013). Consequently, parameterizing and initializing these models for large areas can be difficult (Bugmann, 2001; Stadelmann et al., 2019). Moreover, despite their process-based nature, the mechanisms they use might not generalize to observed extreme events, such as droughts (Fischer et al., 2025; Giardina et al., 2025). Also, with the increased availability of empirical data (Wulder et al., 2012), it might be possible to identify patterns that are currently not captured by process-based models.

Most European countries use empirical models for national-scale predictions of wood availability, whereas process-based models remain of limited use for this purpose. Yet, many of these empirical models do not include climate variables, which limits their ability to account for the impacts of climate change and highlights the need for further model development under changing environmental conditions (Barreiro et al., 2016). A major challenge is that models need to predict responses to environmental conditions that fall outside the range of the observed values used for model development (Barnes et al., 2022).

Machine learning (ML) models are increasingly used in forest ecology and to analyze ecosystem responses to water limitation and other environmental stressors (Liu et al., 2018; Giardina et al., 2023), as they can capture non-linear ecological patterns (Ryo and Rillig, 2017). Compared to process-based models, ML models are easier to apply over larger areas because they require less detailed initialization data (Adams et al., 2013; Liu et al., 2018). Empirical models that integrate ML can potentially also capture extreme events better, provided such events are represented with sufficient variability in the data used to develop them (Materia et al., 2024). Additionally, ML frameworks typically separate model fitting from performance assessment (i.e., by splitting the initial data into training, validation and test sets and through cross-validation), providing a more transparent evaluation of out-of-sample predictive performance (Roberts et al., 2017; Yates et al., 2023). Model validation is required before environmental models are applied for management or policymaking (Eker et al., 2018; Rykiel, 1996; Schuwirth et al., 2019). For forest management decisions, this validation should include comparing the predicted values with the observed values not used in model development (Buchman and Shifley, 1983). Hence, the validation approach of ML frameworks is another advantage that does not seem to be fully explored and may be less demanding compared to other approaches (e.g., in process-based models, which require assessing individual processes and their interactions).

Current applications of ML in forest ecology mostly focus on developing component models that predict rates of change, such as the basal area increment of individual trees (Ashraf et al., 2013; Casas-Gómez et al., 2025; Jevšenak and Skudnik, 2021) or the annual volume growth of a stand (Bayat et al., 2021; Hamidi et al., 2021; Tian et al., 2022). However, these models only include trees that remain alive during the observation time. Consequently, approaches that include mortality and forest regeneration have potentially been underexplored. Models that simultaneously predict both positive and negative changes in a forest stand, such as its total basal area and species composition, require further exploration. Capturing these dynamics is essential for carbon accounting, forest management decisions, and projections of timber production.

This paper addresses these gaps by developing and validating an ML model for Swiss forests that integrates stand, site, and climate variables, using data from the Swiss National Forest Inventory (NFI) (WSL, 2025) and the CH2018 climate scenarios (CH2018 Project Team, 2018).

To do this, we chose an Extreme Gradient Boosting (XGBoost) algorithm because of its ability to converge relatively fast, capture the non-linear relationships that characterize forest ecosystems (Messier et al., 2016), and perform well with structured data (Chen and Guestrin, 2016). The model predicts two key indicators of forest development: basal area per hectare, a measure of wood availability, and the broadleaf fraction, a measure of species composition.

To ensure relevance for management and policymaking, we evaluate the model's ability to generalize to future climate conditions using temporally out-of-sample one- and two-step validations against later NFI observations. In these validations, we compare XGBoost with Lasso regression and a persistence baseline. After this short-horizon validation, we apply the model recursively to generate projections until 2099 for Swiss forests.

A limitation of tree-based algorithms such as XGBoost is that they cannot extrapolate beyond the range of the data on which they were trained: outside the observed range of a predictor, their predictions remain constant rather than continuing the underlying trend. In this respect they differ from established forest models such as the process-based ForClim (Huber et al., 2021) and the empirical MASSIMO (Stadelmann et al., 2019), which represent forest dynamics in ways that let them project responses to conditions that lie outside the historically observed range. In this study, we use a persistence baseline as a simple non-extrapolating reference and Lasso regression as a linear empirical reference. Other non-extrapolating projection frameworks, such as the plot-matching approach of Van Deusen and Roesch (2013) and the USDA Forest Service RPA applications (Oswalt et al., 2019), provide another option. We account for the extrapolation constraint of XGBoost by separating short-horizon validations from longer recursive projections, by comparing it with the persistence baseline, and by reporting, for our projections, the percentage of feature values that fall outside the training range.

Forests in Switzerland cover a large elevational and thus environmental gradient ranging from Mediterranean-type Scots-pine–oak forests to temperate spruce–fir–beech forests and subalpine larch–Stone-pine forests (Huber et al., 2021). This variety of ecosystems covers a bio-climatic gradient that is representative of large parts of Europe (Huber et al., 2021).

We will address the following questions: For temporally held-out one- and two-step inventory transitions, how accurately can an XGBoost model predict changes in the basal area and broadleaf fraction of Swiss forests, and how does its performance compare with Lasso regression and a persistence baseline? When the model is applied recursively beyond the validation horizon available from current NFI observations, how do the projections compare with those from established forest models?

2. Materials and methods

All code used in this study, along with instructions for obtaining the data, is available at the public GitHub repository named BABF-forest-forecasting (Rieder, 2026).

2.1. Study area

Forests cover 32% of the total surface area of Switzerland. These forests contain a wide diversity of sites that range from warm lower altitudes to the alpine timberline. This altitude range shapes local climatic conditions that can vary within short distances, influencing the species composition. The resulting diversity of forest structures is reflected in regionally different management strategies and forest functions, with management objectives varying among regions such as the Swiss Plateau, the Pre-Alps, the Alps, and the Jura. Conifer forests make up 43% of the area and dominate the upper montane and subalpine vegetation belts. Broadleaf forests account for 25% and occur mostly at lower altitudes with mixed forests making up the remaining 32%. Within the growing stock, spruce makes up the highest proportion at 44%, followed by beech at 18% and silver fir at 15% (Rigling and Schaffer, 2015).

This diversity of forest types across a relatively small area, combined with steep climatic gradients, makes Switzerland an ideal setting to study forest dynamics. Its well-documented forest management practices and long-term monitoring data further allow insights that are relevant for understanding broader Central European forest trends.

2.2. Data sources

This study used two primary datasets for modeling: forest data from the Swiss NFI (WSL, 2025) and historical and projected climate data from CH2018 (CH2018 Project Team, 2018).

2.2.1. Swiss National Forest Inventory

The Swiss NFI is a long-term program that monitors Swiss forests, with the goal of providing data and information about Swiss forests to different interest groups. The inventory surveys approximately 6500 permanent plots, with measurements starting in 1983. These plots are arranged on a systematic 1.4 km × 1.4 km grid. Each plot is remeasured approximately every 10 years. Since the fourth assessment (2009–2017), the survey has used a continuous design. In this design, a representative subset (panel) containing approximately one ninth of the complete set of plots is surveyed each year (Fischer and Traub, 2019).

The field survey on each plot uses a nested circular design to collect individual tree data. Within an inner circle of $200\,m^2$, all trees with a Diameter at Breast Height (DBH) of 12 cm or greater are recorded. Trees with a DBH of 36 cm or more are sampled in a $500\,m^2$ circle. Core attributes are recorded for each tree, including species, DBH, and status (for example, living or dead). The basal area for an individual tree is calculated from its DBH measurement. These values are then scaled by a plot-specific extrapolation factor, which determines the weight of individual trees and accounts for variable plot sizes (e.g., due to roads or clearings). The scaled tree values are then summed at the level of sample plots to obtain the total basal area per hectare, including for plots that were only partially resurveyed. In addition to the field surveys, data from aerial images, a forest road survey, and an interview survey among foresters were used. For instance, management information was derived from the interview survey (Fischer and Traub, 2019).

This study analyzes data from five Swiss NFIs (WSL, 2025): NFI1 (1983–1985), NFI2 (1993–1995), NFI3 (2004–2006), NFI4 (2009–2017), and NFI5 (2018–2024). For the final inventory (NFI5), data are available for 7 of the 9 sampling panels at the time of analysis. The NFI data analyzed are organized into three levels, each counted in a different unit. Site-level data provide constant geographical and topographical information, such as coordinates, elevation, slope, aspect, soil pH, and vegetation belt, for the 4164 plots measured in all five inventories. Stand-level data consist of 20,820 records, one for each of these plots in each of the five inventories, capturing plot characteristics like total basal area per hectare and management intensity. Finally, individual tree-level data include 412,391 single-tree measurements across all inventories, detailing variables such as species codes, individual tree basal area, and extrapolation factors, which are aggregated to the plot level to obtain basal area and broadleaf fraction. To obtain the data, we have signed a contractual agreement with the Swiss Federal Institute for Forest, Snow and Landscape Research (WSL).

Not all of these records could be used for modeling. After removing records with missing site, stand, or tree data and records with implausible basal area values, the final dataset comprises 19,659 records from 4063 plots (Fig. 1), which yield the 15,516 inventory transitions used for training and evaluation. The individual exclusion steps are described in Appendix A.

2.2.2. CH2018 climate scenarios for Switzerland (CH2018)

The CH2018 climate scenarios are climate projections for Switzerland created to support impact research and adaptation decisions. The scenarios are derived from the Coordinated Regional Climate Downscaling Experiment, a project that uses an ensemble of regional climate models, which dynamically downscale projections from multiple global climate models to a higher resolution of 12 km or 50 km. The projections cover three different future emission scenarios, known as Representative Concentration Pathways (RCPs): RCP2.6, a strong mitigation scenario consistent with limiting global warming to below 2°C; RCP4.5, an intermediate scenario; and RCP8.5, a high-emission scenario with unabated emissions (CH2018, 2018).

This study uses the CH2018 DAILY-GRIDDED product (CH2018 Project Team, 2018), a dataset that provides transient daily time series from 1981 to 2099 on a regular 2 km × 2 km grid covering Switzerland. The dataset includes daily mean, maximum, and minimum temperatures, as well as the daily precipitation sum. These variables are available for each simulation within a multi-model ensemble, which consists of 12 simulations for RCP2.6, 25 for RCP4.5, and 31 for RCP8.5 (Kotlarski and Rajczak, 2018). The data are freely available under the CC BY 4.0 license.

2.3. Data processing and integration

Data from the Swiss NFI and CH2018 climate scenarios were integrated to create a unified dataset with consistent spatial and temporal alignment. Stand-level records provided the *Basal Area*, while individual tree data were aggregated to calculate the *Broadleaf Fraction*. These variables served as the basis for the target variables and were complemented by derived climate and site predictors.

For the climate predictors, daily CH2018 data were first converted to yearly metrics for each simulation and grid cell. For each RCP, these yearly metrics were then averaged across the available ensemble members, resulting in one ensemble-mean value per year and 2 km × 2 km grid cell. Each NFI plot was linked to the nearest CH2018 grid point via a nearest-neighbor join (Van den Bossche et al., 2024). The plot-level climate features were computed by averaging the yearly ensemble-mean values from the linked grid point over the plot-specific interval between two consecutive NFI measurements and assigning this interval mean to the NFI record at the start of the interval.

The final set of predictor and target variables is summarized in Table 1, with detailed definitions provided in Appendix C. The spatial distribution of the 4063 plots included in the final model dataset is shown in Fig. 1. Additional details on data processing are provided in Appendix A.

2.4. Modeling approach

We use an XGBoost model to predict two target variables for the subsequent inventory period: *Next Basal Area* and *Next Broadleaf Fraction*. XGBoost is a supervised learning algorithm based on an ensemble of decision trees (Cherif and Kortebi, 2019). The model is trained by minimizing an objective function that balances a loss function to measure predictive error against a regularization term to control model complexity (Chen and Guestrin, 2016; Cherif and Kortebi, 2019).

Let $\{(x_i, y_i)\}_{i=1}^{n}$ denote the training data with n training instances, where $x_i \in \mathbb{R}^p$ is the feature vector, where p is the number of features,

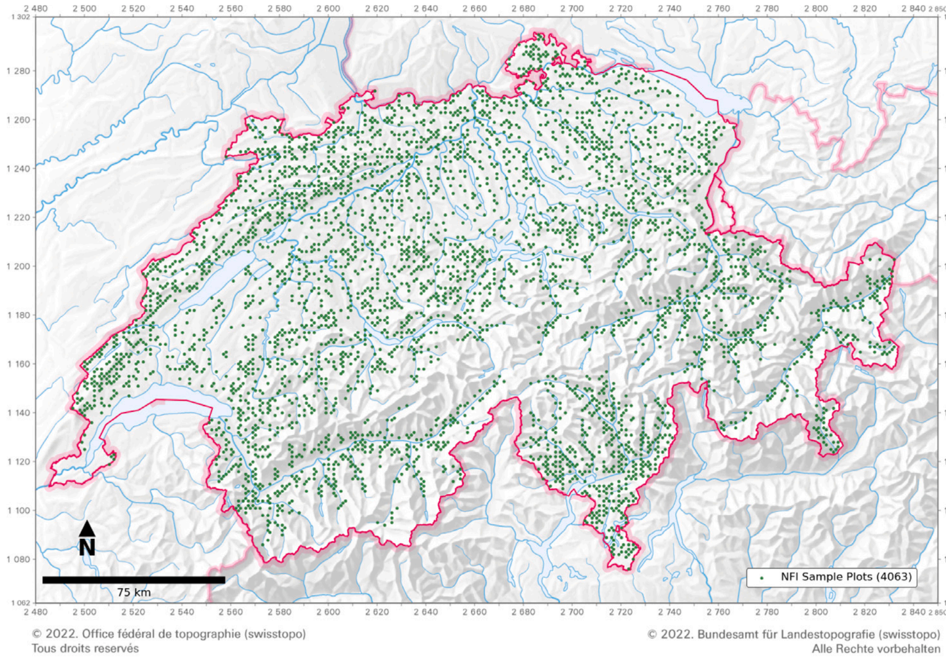

Fig. 1. Spatial distribution of the 4063 sample plots from the Swiss NFI that have been used in the final model of this study. The plot locations are overlaid on a relief map of Switzerland with the national border highlighted. Data sources: NFI (WSL) (WSL, 2025), Federal Office of Topography (swisstopo) (Federal Office of Topography (swisstopo), 2024a,b).

Table 1
Summary of predictor and target variables used in the forest development models. Statistics are computed from the NFI1–NFI5 data (1983–2024, n = 19,659 observations). Values show the median [Q_{25}, Q_{75}], where Q_{25} and Q_{75} are the 25th and 75th percentiles. See Table C.5 for full variable definitions.

Variable	Unit	Median [Q_{25}, Q_{75}]
Predictor Variables: NFI Site & Stand (WSL, 2025)		
Basal Area	m^2/ha	30.9 [19.5, 43.4]
Aspect	Degrees (°)	177.3 [89.9, 292.4]
Slope	Percent (%)	42.6 [21.9, 63.6]
Soil pH	pH value	4.93 [3.77, 6.52]
Elevation	m a.s.l.	981 [655, 1364]
Broadleaf Fraction	Fraction (0–1)	0.21 [0.00, 0.76]
Time Difference	Years	9 [9, 10]
Management Intensity	Cat. code (1–3)	–
Vegetation Belt	Cat. code (1–10)	–
Predictor Variables: Climate (CH2018 Project Team, 2018)		
Mean Minimum Temperature	°C	3.8 [2.0, 5.1]
Variance Minimum Temperature	°C^2	45.4 [44.1, 47.2]
Mean Temperature	°C	7.6 [5.7, 9.1]
Variance Mean Temperature	°C^2	54.5 [51.1, 57.0]
Mean Maximum Temperature	°C	12.0 [9.9, 13.7]
Variance Maximum Temperature	°C^2	69.8 [62.5, 77.1]
Mean Precipitation Sum	mm/year	1324 [1109, 1630]
Variance Precipitation Sum	(mm/day)^2	53.5 [39.6, 77.3]
Mean Dry Days Count	Days/year	223.6 [212.6, 240.9]
Mean Frost Days Count	Days/year	113.6 [91.8, 142.0]
Mean Growing Degree Days	°C·days/year	1744 [1289, 2124]
Target Variables (WSL, 2025)		
Next Basal Area	m^2/ha	31.5 [20.0, 44.0]
Next Broadleaf Fraction	Fraction (0–1)	0.23 [0.00, 0.77]

and $y_i \in \mathbb{R}$ is the observed target. Then, when the squared error is used as the loss function, the objective function is:

$$\mathcal{L}(\{f_k\}_{k=1}^{K}) = \underbrace{\sum_{i=1}^{n}(y_i - \hat{y}_i)^2}_{\text{Loss}} + \underbrace{\sum_{k=1}^{K}\Omega(f_k)}_{\text{Regularization}} . \quad (1)$$

where K is the number of trees and the model's prediction, $\hat{y}_i$, is an aggregation of the outputs from all trees: $\hat{y}_i = \sum_{k=1}^{K} f_k(x_i)$. Each f_k is a tree in the space of regression trees. For a given tree f_k with T_k leaves and leaf weights $\{c_{k,j}\}_{j=1}^{T_k}$, the tree output is $f_k(x_i) = c_{k,q_k(x_i)}$, where $q_k : \mathbb{R}^p \to \{1, \ldots, T_k\}$ maps x_i to a leaf index. The regularization term for a single tree is:

$$\Omega(f_k) = \gamma T_k + \alpha \sum_{j=1}^{T_k} |c_{k,j}| + \frac{1}{2}\lambda \sum_{j=1}^{T_k} c_{k,j}^2, \quad (2)$$

where the hyperparameters γ, λ, and α control penalties on tree complexity. See Appendix D for the definition of the hyperparameters and their optimization. We used the Python implementation of XGBoost provided by the `xgboost` package (Chen and Guestrin, 2016).

We compared the XGBoost model against two reference models. The first is a Lasso regression, a linear model that serves as an interpretable empirical comparator. It was fitted to the same predictors after standardization, with the strength of its ℓ_1 penalty tuned using the same forward split as the XGBoost hyperparameters (see Appendix D). The second is a persistence baseline, a naive non-extrapolating reference that predicts no change between inventories. That is, it carries the observed current state forward, using the current *Basal Area* and *Broadleaf Fraction* as the predictions of *Next Basal Area* and *Next Broadleaf Fraction*. Because the persistence baseline never produces values outside the observed range, it provides a non-extrapolating reference against which the behavior of XGBoost and Lasso can be judged. We used the Lasso and standardization implementations provided by the `scikit-learn` package (Pedregosa et al., 2011).

The predictions of all three models were clipped to ecologically valid ranges. Predicted *Next Basal Area* values were clipped to the range [0,100]. Predicted *Next Broadleaf Fraction* values were clipped to the range [0, 1].

2.5. Model training and evaluation

A separate XGBoost model was trained for each target variable, i.e., one for predicting *Next Basal Area*, and one for *Next Broadleaf Fraction*. Throughout, we refer to a pair consisting of an inventory that provides the predictor state and the subsequent inventory that provides the target as an inventory transition (e.g., the NFI3–NFI4 transition uses the NFI3 plot state to predict the subsequent NFI4 state). The models were evaluated on a temporal split, so that each model is evaluated on inventory transitions occurring later in time than those used for training. This approach is used because predictive models should be validated with future data that were not used in model development (Rykiel, 1996). Random cross-validation was also considered but is not appropriate for a forecast model, as temporal autocorrelation would make the evaluation metrics overly optimistic (Roberts et al., 2017).

We assessed the models on two held-out one-step evaluations to test whether their predictive skill is robust across horizons. In the first, the models were fitted to the NFI1–NFI2 and NFI2–NFI3 transitions and evaluated on the held-out NFI3–NFI4 transition. In the second, they were fitted to the NFI1–NFI2, NFI2–NFI3, and NFI3–NFI4 transitions and evaluated on the held-out NFI4–NFI5 transition. In both, the models predict only the inventory that immediately follows their training data, so both are one-step predictions.

The projections to 2099 (Section 2.7), in contrast, apply the model recursively by feeding each prediction back as the input for the next step. To assess how the prediction error accumulates under this recursive application, we added a recursive two-step evaluation. The model fitted to the NFI1–NFI2 and NFI2–NFI3 transitions first predicted the NFI4 state from the observed NFI3 state, and then predicted the NFI5 state from its own predicted NFI4 state. This two-step prediction of NFI5 was compared with the observed NFI5. In all evaluations, the XGBoost model was compared with the Lasso regression and the persistence baseline on the same held-out data.

To test whether the RMSE differences between these models were larger than expected from sampling variability, we compared each model pair with a spatial block bootstrap of the per-plot RMSE difference (Lahiri, 2013; Brenning, 2012). For each comparison we report the difference in RMSE, with its 95% bootstrap confidence interval; the full procedure and results are given in Appendix E.2.4.

Because of the continuous design of the Swiss NFI, some data leakage is possible. For example, one instance in the training data could have features from 2008 and targets from 2018, while an instance in the test set could have features from 2012 and targets from 2022, causing an overlap in these periods. To assess this problem, we performed a leakage-free sensitivity analysis, in which the model was fitted only to the NFI1–NFI2 and NFI2–NFI3 transitions, so that the last training target measurement preceded the first measurement in the NFI4–NFI5 test transition. The results of this sensitivity analysis are reported in Appendix E.2.1.

The models were trained using RCP4.5 climate data. Since RCP scenarios follow the same historical forcing and differ over the training period only through internal climate model variability, this choice is not expected to substantially affect performance. To test whether it did, we repeated the NFI4–NFI5 one-step evaluation with RCP2.6 and RCP8.5 climate inputs, keeping all other training and test splits constant. The results of this sensitivity analysis are reported in Appendix E.2.2.

2.6. Evaluation metrics and diagnostics

Model accuracy was quantified using the following metrics: coefficient of determination (R^2), root mean square error (RMSE) and bias. For the explicit formula of these measures, see Appendix E. Moreover, the importance of features was measured using the *gain* metric, which is the average reduction in the regularized training objective (loss) contributed by a feature across all trees and all splits where it is used (Chen and Guestrin, 2016).

The models were evaluated on both training and testing sets. Following the two held-out one-step evaluations described in Section 2.5, subgroup performance was summarized as the arithmetic mean of their metrics and reported by *Management Intensity* and *Vegetation Belt*. This subgroup analysis was intended to provide insight into potential sources of variation in model performance and to allow comparison with the process-based ForClim model and the empirical MASSIMO model. Because over-stocked stands are most relevant for management and are where the largest errors were expected, we additionally split the results at the 90th percentile of the observed values and report the upper decile separately.

Unless stated otherwise, the reported evaluations used RCP4.5 climate data.

2.7. Generating forest projections

To generate future projections, the model was retrained on all available historical data. Although this process invalidates the previous error estimates, the retrained model is expected to perform better than a model trained on less data (Roberts et al., 2017).

The projections began with the final measured state of each plot from the fifth Swiss NFI inventory (2018–2024). A future timeline was created for each plot, extending to the year 2099. This timeline followed a predefined schedule of time intervals, which is detailed in Table F.28. Because the final NFI5 measurements were taken in different years, the projection intervals differed among plots. The interval length was 9, 10, or 11 years, and each plot was projected in eight steps until 2099. Climate variables for each future interval were calculated from the CH2018 projections using the same interval-averaging procedure as for the historical data.

The model then operated in the recursive feedback loop shown in Fig. 2. *Basal Area* and *Broadleaf Fraction* were initialized from NFI5 observations and updated at each step with the predicted values from the previous interval, clipped to the ranges described above. Climate predictors and *Time Difference* were updated per interval following Table F.28, whereas *Management Intensity*, *Vegetation Belt*, *Aspect*, *Slope*, *Soil pH*, *Elevation* were held fixed at their NFI5 or site-level values. This assumption of static site conditions and management class is a simplification and is a limitation of the long-term projections. To quantify the influence of this assumption, we additionally performed a counterfactual management-intensity sensitivity analysis, in which the

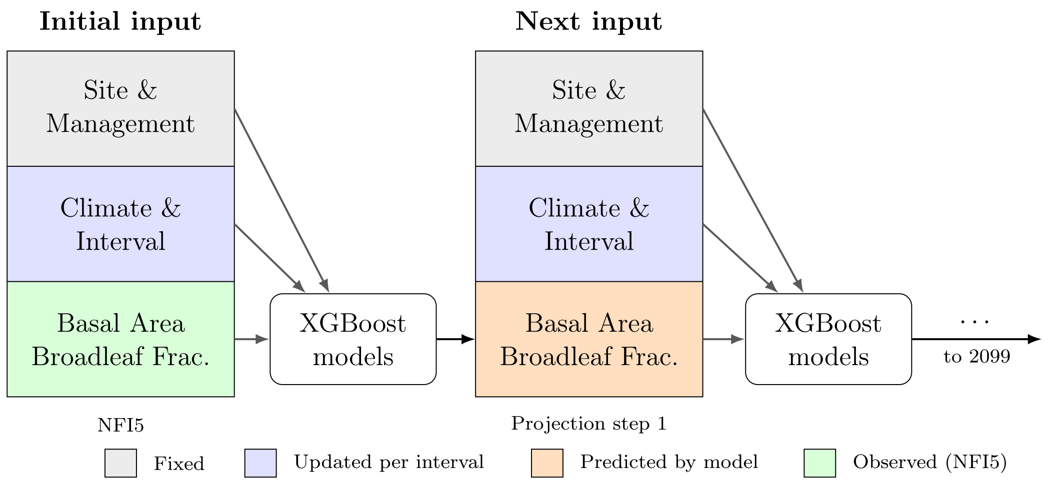

Fig. 2. Recursive projection scheme. The XGBoost models are trained once on all available historical data and remain fixed throughout the projection. At each step, they predict the next Basal Area and Broadleaf Fraction from the current stand state and climate conditions. The predictions become the stand-state inputs for the following step (orange). Site and management inputs remain fixed throughout (gray), climate summaries and the time interval are updated for each projection step (blue). The first step uses observed NFI5 values (green).

projections were re-run with *Management Intensity* held fixed at each of its three classes for all plots (Appendix E.2.3). To account for the randomness in the XGBoost model, the entire simulation was run 100 times, each time with a different random seed.

Because XGBoost cannot extrapolate beyond the range of its training data, we quantified the extrapolation burden of the projections. For each projection step, we computed the percentage of plots for which at least one of the eleven climate predictors fell outside the observed minimum–maximum range of the training data (NFI1–NFI5 under RCP4.5). This diagnostic is reported alongside the projections in Section 3.4 and indicates how far the projected climate inputs move outside the conditions seen during training.

3. Results

This section presents the results from the developed model. Section 3.1 reports the predictive performance of the model on temporally held-out inventory transitions. Section 3.4 shows exploratory projections of future forest development generated with the model under different climate change scenarios.

3.1. Model performance

Across the held-out evaluations, XGBoost achieved the lowest RMSE and the highest R^2 for both target variables (Table 2). For *Next Basal Area*, the RMSE of XGBoost was 10.02 m^2/ha in the direct NFI3–NFI4 evaluation and 10.46 m^2/ha in the direct NFI4–NFI5 evaluation. The corresponding R^2 values were 0.691 and 0.660, respectively. When the model was applied recursively from NFI3 to NFI5, the RMSE increased to 13.33 m^2/ha and the R^2 decreased to 0.443, showing the loss of accuracy when the model is forced to use its own previous prediction as input. For *Next Broadleaf Fraction*, the RMSE was 0.11 and 0.12 in the two direct evaluations, with R^2 values of 0.925 and 0.906. In the recursive two-step evaluation, the RMSE increased to 0.15 and the R^2 decreased to 0.847.

Compared with Lasso and the persistence baseline, the advantage of XGBoost was clearest for *Next Basal Area*. In the direct NFI3–NFI4 evaluation, XGBoost achieved an RMSE of 10.02 m^2/ha, compared with 10.87 m^2/ha for Lasso and 10.78 m^2/ha for the persistence baseline. In the direct NFI4–NFI5 evaluation, the difference between XGBoost and Lasso was smaller, with RMSE values of 10.46 and 10.59 m^2/ha, respectively. For *Next Broadleaf Fraction*, all three models performed relatively well, but XGBoost still had the lowest RMSE in each of the three evaluations. The bias of XGBoost was positive for *Next Basal Area*, ranging from 1.02 to 2.60 m^2/ha, and close to zero for *Next Broadleaf Fraction*.

The good performance of the model can be qualitatively confirmed by plotting the predicted and observed values for the direct NFI4–NFI5 evaluation (Fig. 3). For *Next Basal Area*, the predictions generally follow the 1:1 line, but the agreement is weaker for plots with high observed basal area. This lower accuracy is visible in the upper decile of observed basal area, where the XGBoost RMSE was 17.85 m^2/ha and the R^2 was 0.071 in the NFI4–NFI5 evaluation (Table E.21). For *Next Broadleaf Fraction*, predicted and observed values show a strong positive relationship. At the extremes of 0 and 1, there is clustering along the axes, which is typical for proportions bounded between 0 and 1.

When the two direct one-step evaluations are averaged, XGBoost achieved an RMSE of 10.24 m^2/ha and an R^2 of 0.676 for *Next Basal Area*, and an RMSE of 0.115 and an R^2 of 0.915 for *Next Broadleaf Fraction* (Tables 3 and 4). In this averaged one-step evaluation, the model performed better for unmanaged plots than for managed plots. For *Next Basal Area*, the RMSE was 7.46 m^2/ha for unmanaged plots and 10.57 m^2/ha for managed plots. For *Next Broadleaf Fraction*, the RMSE was 0.058 for unmanaged plots and 0.127 for managed plots. Accuracy also varied across vegetation belts. For *Next Basal Area*, errors were largest in the Lower Montane (N) and Submontane (N) belts and smallest in the Upper Subalpine and Hyperinsubric (S) belts. For *Next Broadleaf Fraction*, the largest errors occurred in the Submontane (N) and Lower Montane (N) belts, whereas errors were small in several high-elevation and southern belts (Tables 3 and 4).

To test whether the RMSE differences between the models were statistically significant rather than a consequence of spatial sampling variability, we compared the models using a spatial block bootstrap (Appendix E.2.4). Across both target variables and all three held-out evaluations, XGBoost achieved a significantly lower RMSE than both the persistence baseline and the Lasso regression: all 95% bootstrap confidence intervals for ΔRMSE excluded zero, and the conclusions were stable across block sizes of 10, 20, and 40 km. For *Next Basal Area* in the recursive two-step evaluation, for example, XGBoost reduced the RMSE by 1.30 m^2/ha (95% CI [1.03, 1.60]) relative to persistence and by 1.00 m^2/ha (95% CI [0.74, 1.27]) relative to Lasso. The advantage of the linear Lasso over the naive persistence baseline was, in contrast, small and inconsistent: it was statistically significant only in the NFI4–NFI5 evaluation, while its confidence interval included zero in the NFI3–NFI4 and the recursive NFI3–NFI5 evaluations (Table E.14).

Table 2
Overview of model performance on held-out inventory-transition evaluations. BA denotes basal area and BF denotes broadleaf fraction. The first direct evaluation is fitted to the NFI1–NFI2 and NFI2–NFI3 transitions and evaluated on the held-out NFI3–NFI4 transition. The recursive evaluation uses the same fitted model, first predicting NFI4 from NFI3 and then predicting NFI5 from the predicted NFI4 state. The second direct evaluation is fitted to the NFI1–NFI2, NFI2–NFI3, and NFI3–NFI4 transitions and evaluated on the held-out NFI4–NFI5 transition.

Training	Test	Model	BA (m^2 ha^{-1})			BF		
			RMSE	R^2	Bias	RMSE	R^2	Bias
NFI1–NFI2 NFI2–NFI3	Direct NFI3–NFI4	XGBoost	10.02	0.691	1.02	0.11	0.925	0.00
		Lasso	10.87	0.636	1.98	0.11	0.917	−0.01
		Persistence	10.78	0.643	−0.25	0.11	0.915	−0.01
	Recursive NFI3–NFI5	XGBoost	13.33	0.443	2.60	0.15	0.847	0.01
		Lasso	14.33	0.356	2.92	0.16	0.837	−0.01
		Persistence	14.63	0.328	−0.11	0.16	0.831	−0.01
NFI1–NFI2 NFI2–NFI3 NFI3–NFI4	Direct NFI4–NFI5	XGBoost	10.46	0.660	1.06	0.12	0.906	0.00
		Lasso	10.59	0.651	1.19	0.12	0.903	0.00
		Persistence	11.18	0.611	0.21	0.13	0.899	−0.01

Table 3
Performance metrics for basal area on the test set. Values are the arithmetic mean of the held-out NFI3–NFI4 evaluation from the model fitted to NFI1–NFI2 and NFI2–NFI3 transitions and the held-out NFI4–NFI5 evaluation from the model fitted to NFI1–NFI2, NFI2–NFI3, and NFI3–NFI4 transitions. Boldface marks the lowest RMSE, highest R^2, and smallest absolute bias within each row.

Section	Group	XGBoost			Lasso			Persistence		
		RMSE	R^2	Bias	RMSE	R^2	Bias	RMSE	R^2	Bias
Overall	All plots	**10.24**	**0.676**	1.04	10.73	0.644	1.59	10.98	0.627	**−0.02**
Decile	Lower 90%	**8.87**	**0.635**	1.09	9.41	0.590	1.91	9.40	0.590	**−0.75**
	Upper decile	**18.38**	**0.131**	**0.62**	18.78	0.094	−1.33	20.23	−0.052	6.58
Management intensity	Managed	**10.57**	**0.637**	1.17	11.05	0.604	1.79	11.48	0.572	**−0.11**
	Rarely managed	**11.47**	**0.618**	**1.42**	11.70	0.602	1.58	12.19	0.568	1.52
	Unmanaged	**7.46**	**0.831**	**0.24**	8.43	0.785	0.88	**7.46**	**0.831**	−1.10
Vegetation belt	Colline with Beech (S) (CO)	7.08	0.832	**0.77**	8.14	0.776	1.80	**6.89**	**0.841**	−0.97
	Colline (CO)	7.66	0.714	1.61	8.59	0.634	3.59	**7.47**	**0.728**	**−0.06**
	Submontane (N) (SM)	**11.39**	**0.474**	1.85	11.80	0.435	3.07	12.75	0.340	**1.49**
	Lower Montane (N) (LM)	**11.78**	**0.585**	1.64	12.13	0.561	1.79	12.88	0.505	**1.05**
	Lower/Upper Montane (S) (MO)	**5.99**	**0.848**	**−0.12**	7.12	0.784	1.09	6.04	0.844	−2.50
	Upper Montane (N) (UM)	**10.48**	**0.686**	0.78	10.77	0.669	0.72	10.79	0.666	**−0.48**
	High-Montane (HM)	**9.29**	**0.751**	**0.46**	9.87	0.719	0.94	9.71	0.729	−0.85
	Subalpine (SA)	**8.52**	**0.803**	**0.25**	9.47	0.756	0.45	8.64	0.797	−1.47
	Upper Subalpine (US)	**4.72**	**0.872**	**−0.23**	6.24	0.779	1.37	5.15	0.846	−2.07
	Hyperinsubric (S) (HY)	**5.55**	**0.768**	**−0.50**	6.21	0.703	1.36	5.57	0.763	−2.71

Table 4
Performance metrics for broadleaf fraction on the test set. Values are the arithmetic mean of the held-out NFI3–NFI4 evaluation from the model fitted to NFI1–NFI2 and NFI2–NFI3 transitions and the held-out NFI4–NFI5 evaluation from the model fitted to NFI1–NFI2, NFI2–NFI3, and NFI3–NFI4 transitions. Boldface marks the lowest RMSE, highest R^2, and smallest absolute bias within each row.

Section	Group	XGBoost			Lasso			Persistence		
		RMSE	R^2	Bias	RMSE	R^2	Bias	RMSE	R^2	Bias
Overall	All plots	**0.115**	**0.915**	**0.002**	0.118	0.910	−0.003	0.120	0.907	−0.008
Decile	Lower 90%	**0.121**	**0.850**	0.006	0.123	0.844	**0.003**	0.127	0.835	−0.012
	Upper decile	**0.076**	**0.112**	−0.019	0.089	−0.210	−0.031	0.082	−0.039	**0.016**
Management intensity	Managed	**0.127**	**0.887**	0.004	0.131	0.881	**0.000**	0.135	0.874	−0.009
	Rarely managed	**0.111**	**0.920**	**0.000**	0.115	0.915	−0.008	0.115	0.914	−0.010
	Unmanaged	0.058	0.982	−0.003	0.063	0.979	−0.011	**0.055**	**0.983**	**0.000**
Vegetation belt	Colline with Beech (S) (CO)	0.032	0.916	−0.012	0.047	0.793	−0.029	**0.020**	**0.970**	**0.002**
	Colline (CO)	**0.089**	**0.932**	**−0.024**	0.091	0.929	−0.034	0.090	0.929	−0.026
	Submontane (N) (SM)	**0.161**	**0.808**	**0.000**	0.164	0.801	−0.005	0.170	0.788	−0.017
	Lower Montane (N) (LM)	**0.140**	**0.836**	**0.003**	0.146	0.822	−0.004	0.150	0.812	−0.012
	Lower/Upper Montane (S) (MO)	0.045	0.979	−0.017	0.063	0.957	−0.039	**0.036**	**0.986**	**0.001**
	Upper Montane (N) (UM)	**0.107**	**0.877**	0.004	0.110	0.869	**0.002**	0.112	0.865	−0.007
	High-Montane (HM)	0.068	0.933	0.007	0.068	0.933	0.004	**0.067**	**0.935**	**0.002**
	Subalpine (SA)	0.030	0.824	0.005	0.030	0.815	0.003	**0.028**	**0.835**	**−0.001**
	Upper Subalpine (US)	0.013	0.763	0.004	0.009	0.861	0.001	**0.008**	**0.893**	**−0.001**
	Hyperinsubric (S) (HY)	0.015	−0.207	−0.011	0.029	−1.264	−0.026	**0.004**	**0.444**	**0.001**

3.2. Sensitivity analyses

We ran two sensitivity analyses to test whether the main NFI4–NFI5 one-step evaluation (Section 2.5) was robust to potential temporal data leakage and to the choice of climate scenario used for training.

In the leakage-free analysis, the model was fitted only to the NFI1–NFI2 and NFI2–NFI3 transitions, so that no training target overlapped in time with the NFI4–NFI5 test transition. Its performance on the NFI4–NFI5 transition remained close to that of the main model. For *Next Basal Area*, the RMSE increased only marginally from 10.46

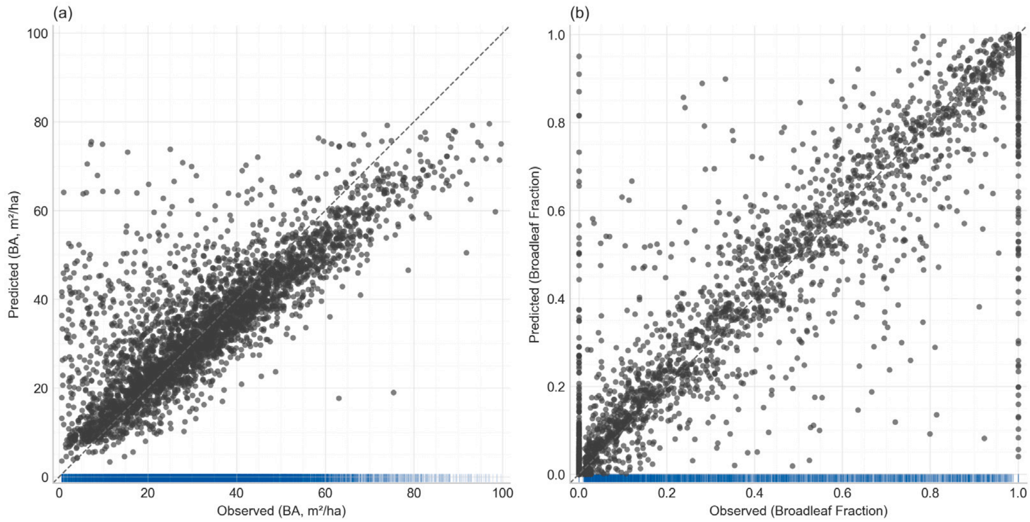

Fig. 3. Observed versus predicted values of the XGBoost model evaluated on the NFI4–NFI5 test transition, for *Next Basal Area* in $m^2 ha^{-1}$ (a) and *Next Broadleaf Fraction* (b). The model was trained on the NFI1–NFI2, NFI2–NFI3, and NFI3–NFI4 transitions under the RCP4.5 climate scenario. The dashed line indicates the 1:1 line of perfect agreement. The horizontal rug at the base of each panel shows the distribution of the respective target variable in the training set.

to 10.54 m^2/ha and the R^2 decreased from 0.660 to 0.655. For *Next Broadleaf Fraction*, the RMSE changed from 0.121 to 0.123 and the R^2 from 0.906 to 0.903 (Table E.11).

The choice of RCP scenario for training had a similarly negligible effect. Repeating the same NFI4–NFI5 evaluation with the model trained under RCP2.6, RCP4.5, or RCP8.5 climate data (fitted to the NFI1–NFI2, NFI2–NFI3, and NFI3–NFI4 transitions) barely changed the test performance. For *Next Basal Area*, the RMSE ranged from 10.460 to 10.463 m^2/ha, and for *Next Broadleaf Fraction* it ranged from 0.121 to 0.122 (Table E.12).

3.3. Feature importance

Feature importance was calculated for the second one-step evaluation, where the models were fitted to the NFI1–NFI2, NFI2–NFI3, and NFI3–NFI4 transitions and evaluated on NFI4–NFI5. The analysis shows that the models relied strongly on the current stand state and broad site gradients. For *Next Basal Area*, the most important predictor was the current *Basal Area* in both the XGBoost and Lasso models (Fig. 4). XGBoost also assigned relatively high importance to *Vegetation Belt* and *Time Difference*, while Lasso concentrated most of its importance on *Basal Area*. For *Next Broadleaf Fraction*, the most important predictor was the current *Broadleaf Fraction* in both models, followed by smaller contributions from *Vegetation Belt* and other site variables (Figure E.12). The climate variables were less important than the stand-state and site variables, but they still contributed to the XGBoost models. In these models, the eleven climate variables together accounted for 14.7% of total XGBoost gain for *Next Basal Area* and 7.4% for *Next Broadleaf Fraction*. The largest individual climate variable was *Variance Precipitation Sum*, with 2.09% and 2.17% of total gain, respectively. In the Lasso models, the combined importance of the climate variables was smaller (3.6% and 1.4%).

3.4. Projected forest development

Projections were generated under three climate scenarios: RCP2.6, RCP4.5, and RCP8.5. Projections start at the state of the forest at NFI5 (2018–2024) and continue until 2099.

Fig. 5 shows projected mean *Basal Area* for managed and unmanaged plots. Unmanaged plots have a higher mean *Basal Area* than managed plots throughout the projection period. Mean *Basal Area* increases in both management groups under all three climate scenarios, but the increase is smaller under stronger climate change. Across all plots, mean *Basal Area* increases from 32.2 m^2/ha at NFI5 to 37.2, 36.4, and 35.8 m^2/ha by 2099 under RCP2.6, RCP4.5, and RCP8.5, respectively. Scenario divergence becomes more pronounced toward the end of the century. The shaded areas show the range across the seed-specific mean projections and widen slightly over time, particularly under the higher-emission scenario RCP8.5.

The lower panel of the projection figures shows how far the climate inputs move outside the historical training range. This fraction remains low under RCP2.6 and RCP4.5, reaching about 1% and 3% of plots, respectively, by the last plotted projection interval. Under RCP8.5, however, the fraction rises to about 30% by the same interval.

Fig. 6 shows projected changes in mean *Basal Area* relative to the starting state at NFI5 for all plots by vegetation belt. The magnitude and direction of change vary across belts. Under RCP4.5, the smallest increases by 2099 are projected for the Lower Montane (N) and Submontane (N) belts, with increases of about 0.5 and 1.1 m^2/ha, respectively. The largest increases are projected for the Upper Subalpine and Lower/Upper Montane (S) belts, with increases of about 11.4 and 10.4 m^2/ha, respectively. The broad pattern is similar across climate scenarios, although RCP8.5 shows smaller increases in several low- to mid-elevation belts than RCP2.6 or RCP4.5. In the Upper Montane (N) belt, the RCP8.5 trajectory flattens after about 2059, peaks around 2079, and then decreases slightly toward the end of the projection period.

The unmanaged-only projection shows a different pattern in the lower northern belts. In unmanaged plots, mean *Basal Area* in the Submontane (N) belt decreases by 6.6, 7.2, and 7.3 m^2/ha by 2099 under RCP2.6, RCP4.5, and RCP8.5, respectively. In the Lower Montane (N) belt, the corresponding decreases are 4.5, 5.9, and 7.1 m^2/ha (Figure F.19). Managed plots in these belts remain above their starting values, so the all-plot means remain positive.

Broadleaf Fraction is projected to increase across Switzerland under all three climate scenarios (Figure F.17). Across all plots, the mean *Broadleaf Fraction* increases from 0.390 at NFI5 to 0.449, 0.463, and 0.479 by 2099 under RCP2.6, RCP4.5, and RCP8.5, respectively. The increase is stronger in managed plots than in unmanaged plots. Under RCP8.5, for example, the mean *Broadleaf Fraction* in managed plots increases by 0.112 by 2099, compared with 0.021 in unmanaged plots. Across vegetation belts, the strongest increase is projected for the Submontane (N) and Lower Montane (N) belts (Fig. 7). Among the remaining belts, a clear increase is projected only for the Upper Montane (N), whereas the other belts remain largely unchanged.

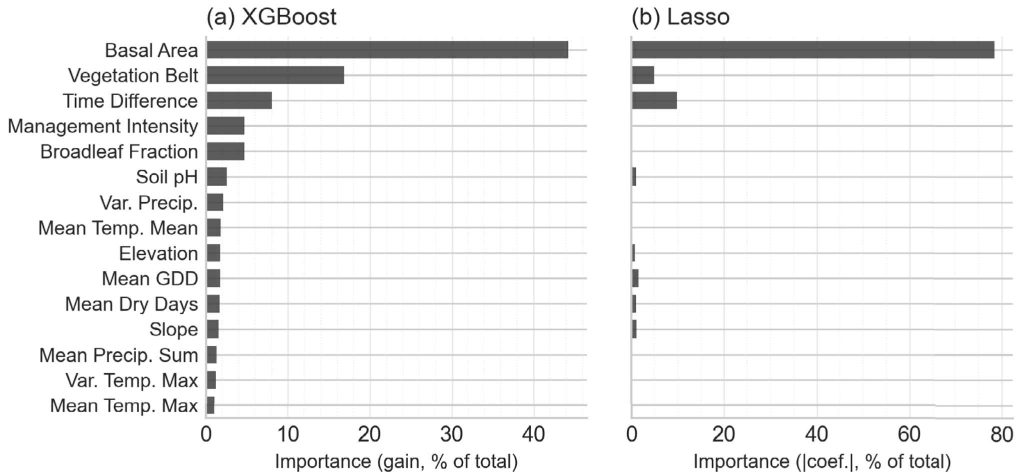

Fig. 4. Predictor importance for *Next Basal Area*, computed for the model trained on the NFI1–NFI2, NFI2–NFI3, and NFI3–NFI4 transitions and evaluated on the NFI4–NFI5 transition under the RCP4.5 climate scenario. XGBoost importance is quantified as the gain metric (average reduction in the regularized training objective per split; panel a), and Lasso importance as the absolute magnitude of the standardized coefficient (panel b). Both are expressed as a percentage of the total across all predictors. The fifteen predictors with the highest XGBoost gain are shown. The two measures quantify importance differently, so equal percentages do not imply equal influence.

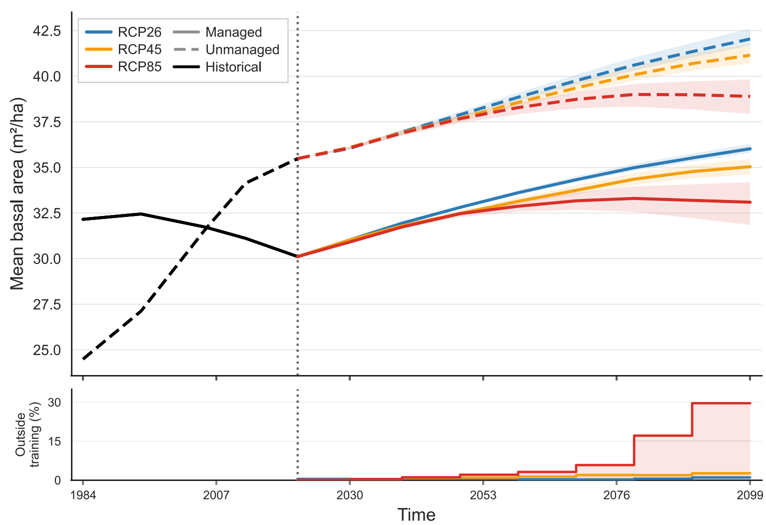

Fig. 5. Projected mean *Basal Area* ($m^2\ ha^{-1}$) from 1983 to 2099, disaggregated by *Management Intensity*: managed plots (solid lines) and unmanaged plots (dashed lines). The black lines show the historical period (NFI1–NFI5); colored lines show projections under RCP2.6, RCP4.5, and RCP8.5 from the starting state of the fifth Swiss NFI inventory (2018–2024). Shaded bands indicate the range across 100 simulation runs. The dotted vertical line marks the start of the projection period. The lower panel shows, for each projected inventory cycle and scenario, the percentage of plots for which at least one of the 11 climate predictors falls outside the observed minimum–maximum range of the training data (NFI1–NFI5 under RCP4.5).

4. Discussion

In this study, we developed a machine-learning model based on the XGBoost algorithm to predict two key indicators of forest development, basal area and broadleaf fraction, from data that national forest inventories routinely collect. We validated the model on temporally held-out inventory transitions and then applied it recursively to project Swiss forests until 2099 under three climate scenarios.

Our main finding is that the model predicts the next-inventory state of a plot accurately for a single inventory step, with high accuracy for broadleaf fraction and medium accuracy for basal area, using only NFI and climate data. Because it does not require detailed parameterization, it is fast to run and can be retrained for other countries with similar data. The principal limitation is that XGBoost cannot extrapolate beyond the range of its training data, and its accuracy declines with each recursive step. The long-term projections to 2099 should therefore be read as exploratory projections rather than validated forecasts, and we use them mainly to compare the direction of change with established forest models.

4.1. Predictive accuracy and operational benefits

The model achieves a medium R^2 for basal area and a high R^2 for broadleaf fraction in the direct one-step evaluations. This performance is partly explained by the strong temporal autocorrelation of both variables between consecutive inventories (Figure B.9). Consistent with this, the feature-importance analysis shows that the current basal area and broadleaf fraction are the most important predictors of their own future values (Figs. 4 and E.12). Beyond the current stand state, vegetation belt was one of the most important predictors, especially in the XGBoost models. This suggests that it captures broad elevational,

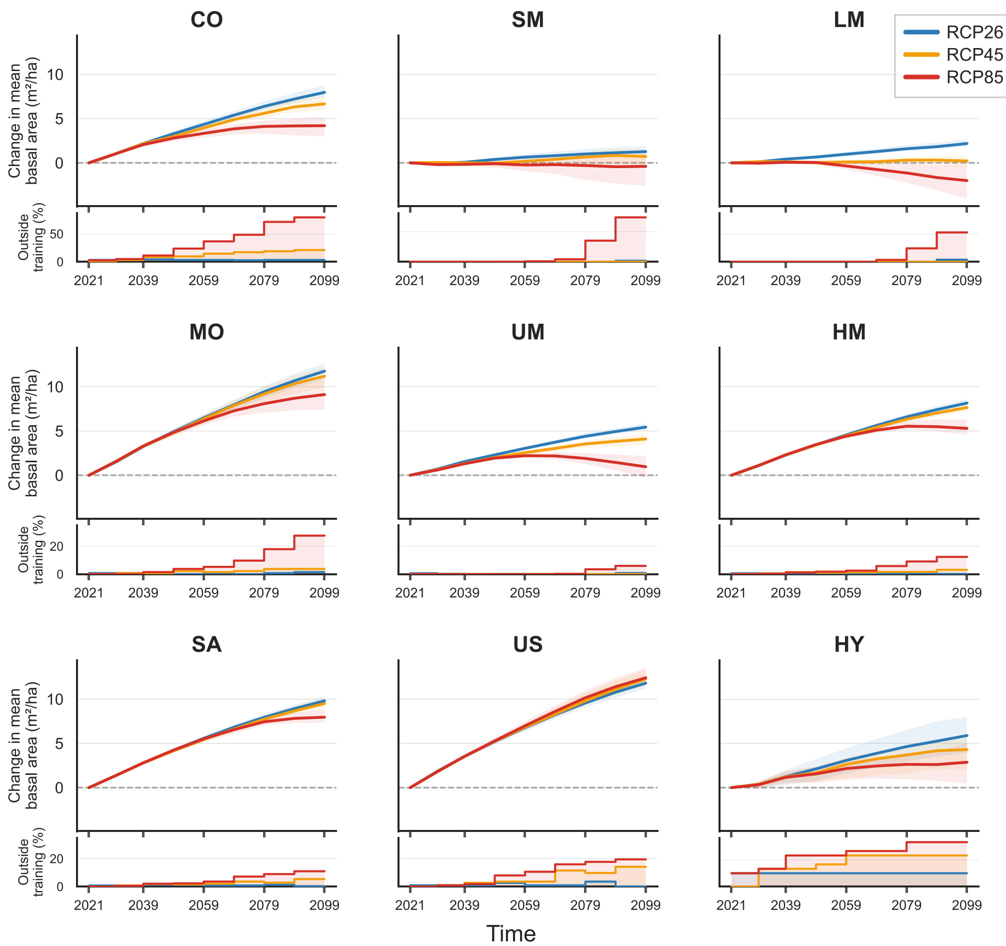

Fig. 6. Projected change in mean *Basal Area* ($m^2\,ha^{-1}$) relative to the starting state of the fifth Swiss NFI inventory (2018–2024), shown separately for each *Vegetation Belt* (CO: Colline, SM: Submontane, LM: Lower Montane N, MO: Lower/Upper Montane S, UM: Upper Montane N, HM: High-Montane, SA: Subalpine, US: Upper Subalpine, HY: Hyperinsubric S) across all plots. Colored lines show the mean change under RCP2.6, RCP4.5, and RCP8.5, averaged over 100 simulation runs; shaded bands indicate the range across runs. The dashed horizontal line marks zero change. The lower panel shows, for each projected inventory cycle and scenario, the percentage of plots for which at least one of the 11 climate predictors falls outside the observed minimum–maximum range of the training data per vegetation belt (NFI1–NFI5 under RCP4.5).

climatic, and ecological gradients across Swiss forests. Individual climate variables had much lower importance, although their combined contribution indicates that climate information still added predictive signal.

Because the current state is so informative, a simple persistence baseline that carries the observed value forward is already a strong reference, especially for broadleaf fraction. In the direct NFI4–NFI5 evaluation, persistence alone reaches an R^2 of 0.899 for broadleaf fraction, and XGBoost improves this only modestly to 0.906. For basal area the advantage of XGBoost is larger (R^2 0.611 to 0.660). A spatial block bootstrap confirms that XGBoost has a significantly lower RMSE than both persistence and Lasso across all held-out evaluations, whereas Lasso improves on persistence only inconsistently (Table E.14). The advantage of XGBoost over the linear Lasso is small in the direct one-step evaluations but grows in the recursive two-step evaluation, where XGBoost retains more accuracy (basal-area R^2 0.443 versus 0.356). For applications where transparency and direct interpretability are more important than small gains in predictive accuracy, however, a linear model may still be preferable.

The model is less accurate for managed plots than for unmanaged plots. This lower accuracy may reflect unobserved management interventions, which are not explicitly represented in the model and can introduce variability beyond what the available predictors capture. For basal area, the RMSE is 10.57 m^2/ha for managed plots compared with 7.46 m^2/ha for unmanaged plots, and for broadleaf fraction it is 0.127 compared with 0.058, indicating that both variables are harder to predict where management is active. A similar pattern was reported by Tian et al. (2022), who found higher accuracy for unmanaged than for managed plots when estimating stand volume growth with random forests.

Model accuracy is also lower for the most densely stocked plots, with the R^2 dropping to 0.131 and the RMSE rising to 18.38 m^2/ha in the upper decile of observed basal area (Table 3). The model is therefore weakest in the over-stocked stands that are of particular interest for management decisions. Across the full range, however, the prediction bias is low for both variables, so the model does not systematically over- or underestimate change. This suggests that the NFI data were sufficient to calibrate the model well in terms of its mean response.

Accuracy also varies across vegetation belts. For basal area, the held-out RMSE rises from 4.72 m^2/ha in the Upper Subalpine and about 5–6 m^2/ha in the southern belts to 11.39 m^2/ha in the Submontane (N) and 11.78 m^2/ha in the Lower Montane (N) belts, and broadleaf fraction follows the same ordering (Tables 3 and 4). The model is least accurate in the lower-elevation northern belts, which are also the most intensively managed, consistent with the lower accuracy for managed plots noted above. The high-elevation and southern belts, which are less intensively managed and more strongly dominated by a single species, are predicted more accurately. However, for broadleaf fraction in several of these belts, including the Hyperinsubric (S) and Upper

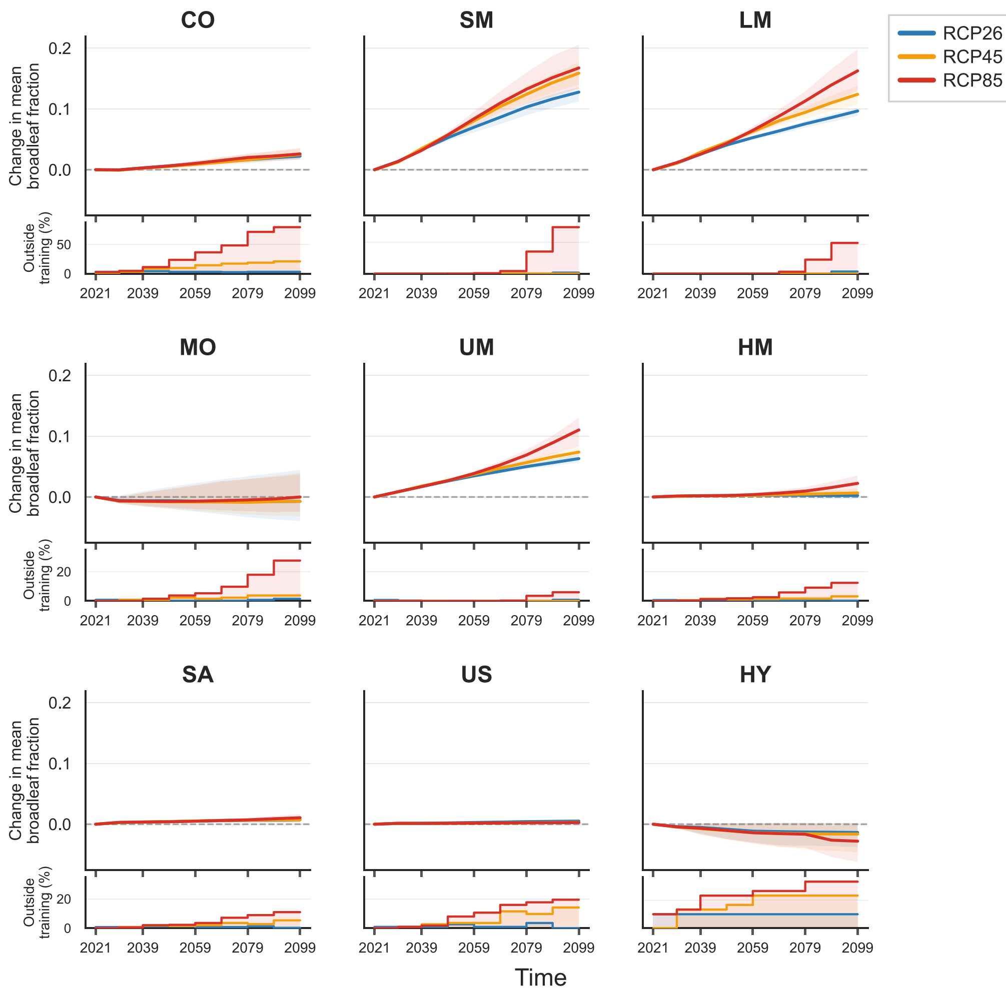

Fig. 7. Projected change in mean *Broadleaf Fraction* relative to the starting state of the fifth Swiss NFI inventory (2018–2024), shown separately for each *Vegetation Belt* (CO: Colline, SM: Submontane, LM: Lower Montane N, MO: Lower/Upper Montane S, UM: Upper Montane N, HM: High-Montane, SA: Subalpine, US: Upper Subalpine, HY: Hyperinsubric S) across all plots. Colored lines show the mean change under RCP2.6, RCP4.5, and RCP8.5, averaged over 100 simulation runs; shaded bands indicate the range across runs. The dashed horizontal line marks zero change. The lower panel shows, for each projected inventory cycle and scenario, the percentage of plots for which at least one of the 11 climate predictors falls outside the observed minimum–maximum range of the training data per vegetation belt (NFI1–NFI5 under RCP4.5).

Subalpine belts, the persistence baseline performs better than XGBoost and Lasso (Table 4). For instance, in the Hyperinsubric (S) belt, the test R^2 is negative for XGBoost (−0.207) and Lasso (−1.264), while persistence reaches 0.444. Both models therefore add nothing over the belt mean, and persistence is the more appropriate reference there.

Based on this performance, we argue that XGBoost and similar tree-based models are most useful when rapid regional- to national-scale projections are needed. Compared with process-based models, they are much faster to set up and run, because they do not require detailed parameterization of physical and biological processes or of management. They also learn complex, non-linear relationships between climate, site conditions, and forest structure directly from data, which can be difficult to represent explicitly in mechanistic frameworks. The partial dependence plots for the climate predictors illustrate this flexibility (Figures E.13 and E.14). However, they remain limited by the quality, coverage, and stationarity of the training data, and their skill declines when they are pushed beyond observed conditions; we return to this in the limitations section.

From a practical perspective, these models can be implemented with established, publicly available open-source libraries, which lowers technical barriers and supports reproducibility. The main requirement is access to a sufficiently long, high-quality time series of inventory data. For Switzerland this was available through a straightforward contractual agreement with the WSL, and comparable NFI datasets exist and are often accessible in other countries, making the approach attractive for national-scale analysis.

4.2. Model projections and comparisons

We applied the trained model recursively to project forest development to the end of the century. Over the next two decades, mean basal area increases under all three climate scenarios. Beyond this period, basal area continues to increase under all scenarios, but more strongly under the milder scenarios than under RCP8.5. Current climate trajectories are estimated to lie between RCP4.5 and RCP8.5 (Lee et al., 2023). Broadleaf fraction is projected to increase under all scenarios, more strongly under stronger climate change and in managed forests.

The projected changes differ among vegetation belts. Across all plots, basal area remains above the NFI5 starting value in all belts by 2099, but the increase is weakest in the lower-elevation northern belts, the Submontane (N) and Lower Montane (N) zones, and strongest at high elevations (Upper Subalpine and Subalpine) and in the southern Lower/Upper Montane (S) belt. Under RCP8.5 the increases in the lower- to mid-elevation northern belts shrink further, and in the Upper Montane (N) belt basal area peaks around 2079 and then declines slightly toward the end of the century. In the unmanaged-only projections, the Submontane (N) and Lower Montane (N) belts fall below their NFI5 starting values under all three scenarios.

The increase in broadleaf fraction is concentrated in the same lower northern belts where basal-area growth is weakest, the Submontane (N), Lower Montane (N), and Upper Montane (N) zones, and is stronger under stronger warming. The southern and high-elevation belts change little in species composition, because they are already broadleaf-dominated or almost purely coniferous and so have little room to shift.

As noted above, the Submontane (N) belt has the highest prediction errors, so its projections should be interpreted most cautiously. Yet the basal-area decline projected for unmanaged plots is consistent with the greater drought exposure of this low-elevation belt, which could push the dominant Norway spruce upslope and lower basal area while alternative species take several decades to migrate in. These remain hypotheses that could be investigated further in process-based or field studies.

We compared these projections with two established models for Swiss forests: the process-based gap model ForClim (Bugmann, 1996) and the empirical model MASSIMO (Stadelmann et al., 2019), which represent the state of the art in forest modeling. Because the models differ in their response variables, spatial units, scenarios, and time horizons, we restrict the comparison to the direction of change; the detailed comparison is given in Appendix F.3.

The direction of the elevational gradient agrees with ForClim (Huber et al., 2021): both models show weakest basal-area development in the lower northern belts and strongest gains toward higher elevations. ForClim simulates decreases in basal area, particularly in the submontane and low montane belts. We also find a decrease in unmanaged and rarely managed plots in these belts, but not in managed plots, for which exploratory projections remain weakly positive. Note that this comparison is limited by the different assumptions of the two models. ForClim simulates managed representative stands and includes process-based responses to soil conditions and species immigration, whereas our projection keeps management class and vegetation belt fixed after NFI5 (see Section 4.3).

The comparison with MASSIMO (Stadelmann et al., 2019; Flury et al., 2024) points in the same direction. MASSIMO projects an overall increase in growing stock under a business-as-usual scenario, consistent with our increasing basal area, and the weakest development in the Plateau region, which is dominated by the submontane and lower montane belts where our model also projects the weakest basal-area increase. Flury et al. (2024) project a rising broadleaf fraction driven partly by a decline in conifers in the intensively managed Plateau and Jura forests, which is consistent with the strong broadleaf shift our model projects in managed plots by 2060 (Figure F.17).

4.3. Limitations and outlook

Static site conditions and management. The model represents forest management only through past management intensity, which is included as a categorical predictor; it does not represent future management scenarios or individual interventions. Site variables, the vegetation belt, and the management class are held constant after NFI5, while only the climate variables, basal area, and broadleaf fraction are updated at each step. Holding these factors constant for 75 years is a simplification, because factors such as the vegetation belt itself shift in response to climate change (Zischg et al., 2021). The model is therefore best suited to regional- to national-scale projections rather than to single plots or to comparing management strategies.

Extrapolation and unvalidated recursion. As a tree-based model, XGBoost cannot extrapolate beyond its training range (Barnes et al., 2022), meaning that outside the observed range of a predictor, its response remains constant rather than extending the underlying trend. The share of plots with at least one climate predictor outside the training range stays small under RCP2.6 and RCP4.5 (about 1% and 3% by the end of the century) but rises to about 30% under RCP8.5 (Fig. 5), so the RCP8.5 projections in particular move into poorly supported climate space. In addition, only the one-step prediction, and a single recursive two-step prediction, could be validated against observed inventories. Accuracy drops clearly after one extra recursive step (basal-area R^2 from 0.660 to 0.443), and the eight steps needed to reach 2099 cannot be validated with currently available data. The long-term projections should therefore be treated as exploratory rather than as validated forecasts.

Mean reversion. A related diagnostic shows that the recursive projections narrow the spread of basal area across plots over time. This was quantified as the standard deviation of basal area across plots within each seed-specific projection. Averaged over the 100 seeds, this standard deviation falls from 18.15 m^2/ha at NFI5 to 8.54, 8.44, and 7.52 m^2/ha by 2099 under RCP2.6, RCP4.5, and RCP8.5, respectively. Such narrowing is the expected behavior of a recursive empirical model that reverts toward the mean of its training data. The projected mean trajectories should therefore be read as conditional means under the fitted model, not as a full account of the variability that disturbance, mortality, regeneration, or changing management could produce.

Uncertainty and outlook. The reported uncertainty captures two sources: the randomness of the XGBoost fit and the spread among climate scenarios. Other sources are not represented. In particular, the data contain few major disturbances such as windstorms, droughts, and bark-beetle outbreaks, so the model may not capture changing disturbance regimes; Monte Carlo simulation could be used to add such sudden changes in forest health and structure. Testing the model on other temperate forests would help assess its generalizability and robustness; because it relies on standardized inventory and climate data, retraining on NFI data from other countries is straightforward. A non-extrapolating projection framework such as the plot-matching approach of Van Deusen and Roesch (2013), used in the USDA Forest Service RPA assessments (Oswalt et al., 2019), would be a natural benchmark for the long-term projections in future work, and space-for-time substitution (Pickett, 1989) could further help represent responses to novel conditions.

5. Conclusion

This study developed an ML model based on the XGBoost algorithm to project forest dynamics in Switzerland. Using data from the Swiss NFI and CH2018 climate scenarios, the model predicts changes in basal area and broadleaf fraction through the end of the century. Projections indicate weaker basal-area development in lower-elevation belts, including decreases in unmanaged Submontane (N) and Lower Montane (N) plots, and stronger increases in high-elevation and southern montane belts, while broadleaf fraction is projected to increase most strongly in the lower northern belts, especially under RCP8.5. However, these belt-level basal-area differences should be interpreted alongside the narrowing of basal-area spread across plots, consistent with mean reversion. These results are broadly consistent in direction with projections from both a process-based model, ForClim, and an empirical model, MASSIMO, although direct comparisons are limited by differences in model structure, target variables, and scenario definitions.

Overall, our findings demonstrate that machine-learning approaches can provide computationally efficient, large-scale projections of forest structure and species composition using widely available inventory and climate data. Future applications may benefit forest ecosystem management by considering ecosystem service indicators as response variables. Future applications may help explore trade-offs and synergies in forest development.

CRediT authorship contribution statement

Dea Rieder: Methodology, Investigation, Formal analysis, Data curation, Conceptualization, Writing – original draft. **Maximiliano Costa:** Writing – review & editing. **Christian Temperli:** Writing – review & editing, Resources. **Francesco Giardina:** Writing – review & editing. **Giacomo Vaccario:** Writing – review & editing, Writing – original draft, Supervision.

Declaration of competing interest

The authors declare that they have no known competing financial interests or personal relationships that could have appeared to influence the work reported in this paper.

Appendix A. Supplementary data

Supplementary material related to this article can be found online at https://doi.org/10.1016/j.ecolmodel.2026.111763.

Data availability

Code and data-access instructions are available in the BABF-forest-forecasting GitHub repository. Swiss NFI data can be obtained from WSL subject to eligibility and a written data-use agreement. CH2018 data are available under the CC BY 4.0 license.

References

Adams, H.D., Williams, A.P., Xu, C., Rauscher, S.A., Jiang, X., McDowell, N.G., 2013. Empirical and process-based approaches to climate-induced forest mortality models. Frontiers in Plant Science 4, 438. http://dx.doi.org/10.3389/fpls.2013.00438.

Allen, C.D., Macalady, A.K., Chenchouni, H., Bachelet, D., McDowell, N., Vennetier, M., Kitzberger, T., Rigling, A., Breshears, D.D., Hogg, E.H.T., Gonzalez, P., Fensham, R., Zhang, Z., Castro, J., Demidova, N., Lim, J.-H., Allard, G., Running, S.W., Semerci, A., Cobb, N., 2010. A global overview of drought and heat-induced tree mortality reveals emerging climate change risks for forests. Forest Ecol. Manag. 259 (4), 660–684. http://dx.doi.org/10.1016/j.foreco.2009.09.001, URL: https://www.sciencedirect.com/science/article/pii/S037811270900615X.

Ashraf, M.I., Zhao, Z., Bourque, C.P.-A., MacLean, D.A., Meng, F.-R., 2013. Integrating biophysical controls in forest growth and yield predictions with artificial intelligence technology. Can. J. Forest Res. 43 (12), 1162–1171. http://dx.doi.org/10.1139/cjfr-2013-0090.

Barnes, C.L., Essington, T.E., Pirtle, J.L., Rooper, C.N., Laman, E.A., Holsman, K.K., Aydin, K.Y., Thorson, J.T., 2022. Climate-informed models benefit hindcasting but present challenges when forecasting species–habitat associations. Ecography 2022 (10), e06189. http://dx.doi.org/10.1111/ecog.06189, URL: https://nsojournals.onlinelibrary.wiley.com/doi/abs/10.1111/ecog.06189, _eprint: https://nsojournals.onlinelibrary.wiley.com/doi/pdf/10.1111/ecog.06189.

Barreiro, S., Schelhaas, M.-J., Kändler, G., Antón-Fernández, C., Colin, A., Bontemps, J.-D., Alberdi, I., Condés, S., Dumitru, M., Ferezliev, A., Fischer, C., Gasparini, P., Gschwantner, T., Kindermann, G., Kjartansson, B., Kovácsevics, P., Kucera, M., Lundström, A., Marin, G., Mozgeris, G., Nord-Larsen, T., Packalen, T., Redmond, J., Sacchelli, S., Sims, A., Snorrason, A., Stoyanov, N., Thürig, E., Wikberg, P.-E., 2016. Overview of methods and tools for evaluating future woody biomass availability in European countries. Ann. For. Sci. 73 (4), 823–837. http://dx.doi.org/10.1007/s13595-016-0564-3.

Bayat, M., Bettinger, P., Hassani, M., Heidari, S., 2021. Ten-year estimation of Oriental beech (Fagus orientalis Lipsky) volume increment in natural forests: a comparison of an artificial neural networks model, multiple linear regression and actual increment. For.: An Int. J. For. Res. 94 (4), 598–609. http://dx.doi.org/10.1093/forestry/cpab001, _eprint: https://academic.oup.com/forestry/article-pdf/94/4/598/39611248/cpab001.pdf.

Van den Bossche, J., Jordahl, K., Fleischmann, M., Richards, M., McBride, J., Wasserman, J., Garcia Badaracco, A., Snow, A.D., Ward, B., Tratner, J., Gerard, J., Perry, M., cjqf, Hjelle, G.A., Taves, M., ter Hoeven, E., Cochran, M., Bell, R., rraymondgh, Bartos, M., Roggemans, P., Culbertson, L., Caria, G., Tan, N.Y., Eubank, N., sangarshanan, Flavin, J., Rey, S., Gardiner, J., 2024. geopandas/geopandas: v1.0.1. http://dx.doi.org/10.5281/zenodo.12625316, Zenodo.

Brecka, A.F.J., Shahi, C., Chen, H.Y.H., 2018. Climate change impacts on boreal forest timber supply. For. Policy Econ. 92, 11–21. http://dx.doi.org/10.1016/j.forpol.2018.03.010, URL: https://www.sciencedirect.com/science/article/pii/S138993411730535X.

Brenning, A., 2012. Spatial cross-validation and bootstrap for the assessment of prediction rules in remote sensing: The R package sperrorest. In: 2012 IEEE International Geoscience and Remote Sensing Symposium. IEEE, pp. 5372–5375.

Brockerhoff, E.G., Barbaro, L., Castagneyrol, B., Forrester, D.I., Gardiner, B., González-Olabarria, J.R., Lyver, P.O., Meurisse, N., Oxbrough, A., Taki, H., et al., 2017. Forest biodiversity, ecosystem functioning and the provision of ecosystem services. Biodivers. Conserv. 26 (13), 3005–3035.

Buchman, R.G., Shifley, S.R., 1983. Guide to evaluating forest growth projection systems. J. For. 81 (4), 232–254. http://dx.doi.org/10.1093/jof/81.4.232, _eprint: https://academic.oup.com/jof/article-pdf/81/4/232/63796818/jof_81_4_232.pdf.

Bugmann, H.K.M., 1996. A simplified forest model to study species composition along climate gradients. Ecology 77 (7), 2055–2074. http://dx.doi.org/10.2307/2265700, URL: https://esajournals.onlinelibrary.wiley.com/doi/abs/10.2307/2265700, _eprint: https://esajournals.onlinelibrary.wiley.com/doi/pdf/10.2307/2265700.

Bugmann, H., 2001. A review of forest gap models. Clim. Change 51 (3), 259–305. http://dx.doi.org/10.1023/A:1012525626267.

Bugmann, H., Seidl, R., 2022. The evolution, complexity and diversity of models of long-term forest dynamics. J. Ecol. 110 (10), 2288–2307. http://dx.doi.org/10.1111/1365-2745.13989, URL: https://besjournals.onlinelibrary.wiley.com/doi/abs/10.1111/1365-2745.13989, _eprint: https://besjournals.onlinelibrary.wiley.com/doi/pdf/10.1111/1365-2745.13989.

Casas-Gómez, P., Torres, J.F., Linares, J.C., Troncoso, A., Martínez-Álvarez, F., 2025. Forecasting basal area increment in forest ecosystems using deep learning: A multi-species analysis in the Himalayas. Ecol. Informatics 85, 102951. http://dx.doi.org/10.1016/j.ecoinf.2024.102951, URL: https://www.sciencedirect.com/science/article/pii/S157495412400493X.

CH2018, 2018. CH2018 – Climate Scenarios for Switzerland, Technical Report. Technical Report, National Centre for Climate Services (NCCS), Zurich.

CH2018 Project Team, 2018. CH2018 – Klimaszenarien für die Schweiz. National Centre for Climate Services (NCCS), Place: Zurich, Switzerland, Published: Dataset, Version 1.0, DOI: 10.18751/Climate/Scenarios/CH2018/1.0.

Chen, T., Guestrin, C., 2016. XGBoost: A scalable tree boosting system. In: Proceedings of the 22nd ACM SIGKDD International Conference on Knowledge Discovery and Data Mining. KDD '16, Association for Computing Machinery, New York, NY, USA, pp. 785–794. http://dx.doi.org/10.1145/2939672.2939785.

Cherif, I.L., Kortebi, A., 2019. On using eXtreme gradient boosting (XGBoost) machine learning algorithm for home network traffic classification. In: 2019 Wireless Days (WD). pp. 1–6. http://dx.doi.org/10.1109/WD.2019.8734193.

Eker, S., Rovenskaya, E., Obersteiner, M., Langan, S., 2018. Practice and perspectives in the validation of resource management models. Nat. Commun. 9 (1), 5359. http://dx.doi.org/10.1038/s41467-018-07811-9.

Elkin, C., Gutiérrez, A.G., Leuzinger, S., Manusch, C., Temperli, C., Rasche, L., Bugmann, H., 2013. A 2°C warmer world is not safe for ecosystem services in the European Alps. Global Change Biol. 19 (6), 1827–1840.

Federal Office of Topography (swisstopo), 2024a. Overview maps of Switzerland (Übersichtskarten der Schweiz). URL: https://www.swisstopo.admin.ch/de/ubersichtskarten-der-schweiz, Place: Wabern, Switzerland, Published: Web page, URL: https://www.swisstopo.admin.ch/de/ubersichtskarten-der-schweiz, Accessed: 2025-07-16.

Federal Office of Topography (swisstopo), 2024b. swissBOUNDARIES3D: Administrative boundaries of Switzerland and Liechtenstein. URL: https://www.swisstopo.admin.ch/en/landscape-model-swissboundaries3d, Place: Wabern, Switzerland, Published: Webpage, URL: https://www.swisstopo.admin.ch/en/landscape-model-swissboundaries3d, Accessed: 2025-07-16.

Fischer, R., Anders, T., Bugmann, H., Djahangard, M., Dreßler, G., Hetzer, J., Hickler, T., Hiltner, U., Marano, G., Sperlich, D., Yousefpour, R., Knapp, N., 2025. Perspectives for forest modeling to improve the representation of drought-related tree mortality. Journal für Kulturpflanzen 77 (2), 50–69. http://dx.doi.org/10.5073/JfK.2025.02.05.

Fischer, C., Traub, B., 2019. Swiss National Forest Inventory – Methods and Models of the Fourth Assessment. http://dx.doi.org/10.1007/978-3-030-19293-8.

Flury, R., Portier, J., Rohner, B., Baltensweiler, A., Di Bella Meusburger, K., Scherrer, D., Thürig, E., Stadelmann, G., 2024. Soil and climate-dependent ingrowth inference: broadleaves on their slow way to conquer Swiss forests. Ecography 2024 (7), e07174.

Fontes, L., Bontemps, J.-D., Bugmann, H., Van Oijen, M., Gracia, C., Kramer, K., Lindner, M., Rötzer, T., Skovsgaard, J.P., 2010. Models for supporting forest management in a changing environmental. For. Syst. 19 (1), 8–29.

Giardina, F., Gentine, P., Konings, A.G., Seneviratne, S.I., Stocker, B.D., 2023. Diagnosing evapotranspiration responses to water deficit across biomes using deep learning. New Phytol. 240 (3), 968–983.

Giardina, F., Padrón, R.S., Stocker, B.D., Schumacher, D.L., Seneviratne, S.I., 2025. Large biases in the frequency of water limitation across Earth system models. Commun. Earth & Environ. 6 (1), 469.

Gustafson, E.J., 2013. When relationships estimated in the past cannot be used to predict the future: using mechanistic models to predict landscape ecological dynamics in a changing world. Landsc. Ecol. 28 (8), 1429–1437.

Hamidi, S.K., Zenner, E.K., Bayat, M., Fallah, A., 2021. Analysis of plot-level volume increment models developed from machine learning methods applied to an uneven-aged mixed forest. Ann. For. Sci. 78 (1), 4. http://dx.doi.org/10.1007/s13595-020-01011-6.

Henne, P.D., Bigalke, M., Büntgen, U., Colombaroli, D., Conedera, M., Feller, U., Frank, D., Fuhrer, J., Grosjean, M., Heiri, O., Luterbacher, J., Mestrot, A., Rigling, A., Rössler, O., Rohr, C., Rutishauser, T., Schwikowski, M., Stampfli, A., Szidat, S., Theurillat, J.-P., Weingartner, R., Wilcke, W., Tinner, W., 2018. An empirical perspective for understanding climate change impacts in Switzerland. Reg. Environ. Chang. 18 (1), 205–221. http://dx.doi.org/10.1007/s10113-017-1182-9.

Huber, N., Bugmann, H., Cailleret, M., Bircher, N., Lafond, V., 2021. Stand-scale climate change impacts on forests over large areas: transient responses and projection uncertainties. Ecol. Appl. 31 (4), e02313.

Iverson, L.R., McKenzie, D., 2013. Tree-species range shifts in a changing climate: detecting, modeling, assisting. Landsc. Ecol. 28 (5), 879–889. http://dx.doi.org/10.1007/s10980-013-9885-x.

Jevšenak, J., Skudnik, M., 2021. A random forest model for basal area increment predictions from national forest inventory data. Forest Ecol. Manag. 479, 118601. http://dx.doi.org/10.1016/j.foreco.2020.118601, URL: https://www.sciencedirect.com/science/article/pii/S0378112720313700.

Keenan, R.J., 2015. Climate change impacts and adaptation in forest management: a review. Ann. For. Sci. 72 (2), 145–167.

Kotlarski, S., Rajczak, J., 2018. CH2018 - Climate Scenarios for Switzerland: Documentation of the Localized CH2018 Datasets. Technical Report, National Centre for Climate Services (NCCS), Zurich.

Krieger, D.J., 2001. Economic Value of Forest Ecosystem Services: A Review. The Wilderness Society.

Krug, J.H.A., 2018. Accounting of GHG emissions and removals from forest management: a long road from Kyoto to Paris. Carbon Balance Manag. 13 (1), 1. http://dx.doi.org/10.1186/s13021-017-0089-6.

Lahiri, S.N., 2013. Resampling Methods for Dependent Data. Springer Science & Business Media.

Lee, H., Calvin, K., Dasgupta, D., Krinner, G., Mukherji, A., Thorne, P., Trisos, C., Romero, J., Aldunce, P., Barret, K., et al., 2023. IPCC, 2023: Climate change 2023: Synthesis report, summary for policymakers. Contribution of working groups i, II and III to the sixth assessment report of the intergovernmental panel on climate change [core writing team, h. Lee and j. romero (eds.)]. IPCC, geneva, Switzerland. Intergovernmental Panel on Climate Change (IPCC).

Liu, Z., Peng, C., Work, T., Candau, J.-N., DesRochers, A., Kneeshaw, D., 2018. Application of machine-learning methods in forest ecology: recent progress and future challenges. Environ. Rev. 26 (4), 339–350.

Mäkelä, A., Landsberg, J., Ek, A.R., Burk, T.E., Ter-Mikaelian, M., Ågren, G.I., Oliver, C.D., Puttonen, P., 2000. Process-based models for forest ecosystem management: current state of the art and challenges for practical implementation. Tree Physiol. 20 (5–6), 289–298.

Materia, S., García, L.P., van Straaten, C., Sungmin, O., Mamalakis, A., Cavicchia, L., Coumou, D., de Luca, P., Kretschmer, M., Donat, M., 2024. Artificial intelligence for climate prediction of extremes: State of the art, challenges, and future perspectives. Wiley Interdiscip. Rev.: Clim. Chang. 15 (6), e914.

Messier, C., Puettmann, K., Filotas, E., Coates, D., 2016. Dealing with non-linearity and uncertainty in forest management. Curr. For. Rep. 2 (2), 150–161. http://dx.doi.org/10.1007/s40725-016-0036-x.

Oswalt, S.N., Smith, W.B., Miles, P.D., Pugh, S.A., 2019. Forest resources of the United States, 2017: A technical document supporting the Forest Service 2020 RPA Assessment. Gen. Tech. Rep. WO-97, 97.

Pedregosa, F., Varoquaux, G., Gramfort, A., Michel, V., Thirion, B., Grisel, O., Blondel, M., Prettenhofer, P., Weiss, R., Dubourg, V., Vanderplas, J., Passos, A., Cournapeau, D., Brucher, M., Perrot, M., Duchesnay, E., 2011. Scikit-learn: Machine learning in Python. J. Mach. Learn. Res. 12, 2825–2830.

Peñuelas, J., Boada, M., 2003. A global change-induced biome shift in the Montseny mountains (NE Spain). Global Change Biol. 9 (2), 131–140. http://dx.doi.org/10.1046/j.1365-2486.2003.00566.x, URL: https://onlinelibrary.wiley.com/doi/abs/10.1046/j.1365-2486.2003.00566.x, _eprint: https://onlinelibrary.wiley.com/doi/pdf/10.1046/j.1365-2486.2003.00566.x.

Piao, S., Wang, X., Ciais, P., Zhu, B., Wang, T., Liu, J., 2011. Changes in satellite-derived vegetation growth trend in temperate and boreal Eurasia from 1982 to 2006. Global Change Biol. 17 (10), 3228–3239. http://dx.doi.org/10.1111/j.1365-2486.2011.02419.x.

Pickett, S.T., 1989. Space-for-time substitution as an alternative to long-term studies. In: Long-Term Studies in Ecology: Approaches and Alternatives. Springer, pp. 110–135.

Rieder, D., 2026. BABF-forest-forecasting (GitHub repository). URL: https://github.com/drdrddrd/BABF-forest-forecasting, commit add project files, URL: https://github.com/drdrddrd/BABF-forest-forecasting. (Accessed 19 June 2026).

Rigling, A., Schaffer, H.P., 2015. Forest report 2015.

Rittenhouse, C.D., Shifley, S.R., Dijak, W.D., Fan, Z., Thompson, F.R., Millspaugh, J.J., Perez, J.A., Sandeno, C.M., 2011. Application of landscape and habitat suitability models to conservation: the Hoosier National Forest land-management plan. In: Landscape Ecology in Forest Management and Conservation. Springer, pp. 299–328.

Roberts, D.R., Bahn, V., Ciuti, S., Boyce, M.S., Elith, J., Guillera-Arroita, G., Hauenstein, S., Lahoz-Monfort, J.J., Schröder, B., Thuiller, W., Warton, D.I., Wintle, B.A., Hartig, F., Dormann, C.F., 2017. Cross-validation strategies for data with temporal, spatial, hierarchical, or phylogenetic structure. Ecography 40 (8), 913–929. http://dx.doi.org/10.1111/ecog.02881, URL: https://nsojournals.onlinelibrary.wiley.com/doi/abs/10.1111/ecog.02881, _eprint: https://nsojournals.onlinelibrary.wiley.com/doi/pdf/10.1111/ecog.02881.

Rykiel, E.J., 1996. Testing ecological models: the meaning of validation. Ecol. Model. 90 (3), 229–244. http://dx.doi.org/10.1016/0304-3800(95)00152-2, URL: https://www.sciencedirect.com/science/article/pii/0304380095001522.

Ryo, M., Rillig, M.C., 2017. Statistically reinforced machine learning for nonlinear patterns and variable interactions. Ecosphere 8 (11), e01976. http://dx.doi.org/10.1002/ecs2.1976, URL: https://esajournals.onlinelibrary.wiley.com/doi/abs/10.1002/ecs2.1976, _eprint: https://esajournals.onlinelibrary.wiley.com/doi/pdf/10.1002/ecs2.1976.

Schuwirth, N., Borgwardt, F., Domisch, S., Friedrichs, M., Kattwinkel, M., Kneis, D., Kuemmerlen, M., Langhans, S.D., Martínez-López, J., Vermeiren, P., 2019. How to make ecological models useful for environmental management. Ecol. Model. 411, 108784. http://dx.doi.org/10.1016/j.ecolmodel.2019.108784, URL: https://www.sciencedirect.com/science/article/pii/S0304380019302923.

Seidl, R., Thom, D., Kautz, M., Martin-Benito, D., Peltoniemi, M., Vacchiano, G., Wild, J., Ascoli, D., Petr, M., Honkaniemi, J., Lexer, M.J., Trotsiuk, V., Mairota, P., Svoboda, M., Fabrika, M., Nagel, T.A., Reyer, C.P.O., 2017. Forest disturbances under climate change. Nat. Clim. Chang. 7 (6), 395–402. http://dx.doi.org/10.1038/nclimate3303.

Senf, C., Pflugmacher, D., Zhiqiang, Y., Sebald, J., Knorn, J., Neumann, M., Hostert, P., Seidl, R., 2018. Canopy mortality has doubled in Europe's temperate forests over the last three decades. Nat. Commun. 9 (1), 4978. http://dx.doi.org/10.1038/s41467-018-07539-6.

Shifley, S.R., He, H.S., Lischke, H., Wang, W.J., Jin, W., Gustafson, E.J., Thompson, J.R., Thompson, F.R., Dijak, W.D., Yang, J., 2017. The past and future of modeling forest dynamics: from growth and yield curves to forest landscape models. Landsc. Ecol. 32 (7), 1307–1325. http://dx.doi.org/10.1007/s10980-017-0540-9.

Stadelmann, G., Temperli, C., Rohner, B., Didion, M., Herold, A., Rösler, E., Thürig, E., 2019. Presenting MASSIMO: A management scenario simulation model to project growth, harvests and carbon dynamics of Swiss forests. Forests 10 (2), http://dx.doi.org/10.3390/f10020094, URL: https://www.mdpi.com/1999-4907/10/2/94.

Taylor, A., 2009. A review of forest succession models and their suitability for forest management planning. For. Sci. -Washington- 55, http://dx.doi.org/10.1093/forestscience/55.1.23.

Temperli, C., Zell, J., Bugmann, H., Elkin, C., 2013. Sensitivity of ecosystem goods and services projections of a forest landscape model to initialization data. Landsc. Ecol. 28 (7), 1337–1352.

Thürig, E., Stadelmann, G., Didion, M., 2021. Estimating Carbon Stock Changes in Living and Dead Biomass and Soil for the Technical Correction of Switzerland's Forest Management Reference Level for the Swiss NIR 2021 (1990–2019) – Modeling Methodology and Results. Technical Report, Swiss Federal Institute for Forest, Snow and Landscape Research (WSL), Birmensdorf, Switzerland, URL: https://www.bafu.admin.ch/bafu/en/home/topics/climate/publications-and-data/publications/estimating-carbon-stock-changes.html.

Tian, H., Zhu, J., He, X., Chen, X., Jian, Z., Li, C., Ou, Q., Li, Q., Huang, G., Liu, C., Xiao, W., 2022. Using machine learning algorithms to estimate stand volume growth of Larix and Quercus forests based on national-scale Forest Inventory data in China. For. Ecosyst. 9, 100037. http://dx.doi.org/10.1016/j.fecs.2022.100037.

Van Deusen, P.C., Roesch, F.A., 2013. Trends and projections from annual forest inventory plots and coarsened exact matching. Math. Comput. For. & Natural-Resource Sci. (MCFNS) 5 (2), 126–134.

Walther, G.-R., 2003. Plants in a warmer world. Perspect. Plant Ecol. Evol. Syst. 6 (3), 169–185. http://dx.doi.org/10.1078/1433-8319-00076, URL: https://www.sciencedirect.com/science/article/pii/S1433831904700748.

Walther, G.-R., Post, E., Convey, P., Menzel, A., Parmesan, C., Beebee, T.J.C., Fromentin, J.-M., Hoegh-Guldberg, O., Bairlein, F., 2002. Ecological responses to recent climate change. Nature 416 (6879), 389–395. http://dx.doi.org/10.1038/416389a.

Wolf, S., Paul-Limoges, E., 2023. Drought and heat reduce forest carbon uptake. Nat. Commun. 14 (1), 6217. http://dx.doi.org/10.1038/s41467-023-41854-x.

WSL, 2025. Schweizerisches Landesforstinventar LFI. Daten der Erhebung(en) 1993-95 / 2004-06 / 2009–2017 / 2018–2024. Christian Temperli. Eidg. Forschungsanstalt WSL, Birmensdorf. WSL.

Wulder, M.A., Masek, J.G., Cohen, W.B., Loveland, T.R., Woodcock, C.E., 2012. Opening the archive: How free data has enabled the science and monitoring promise of Landsat. Remote Sens. Environ. 122, 2–10.

Yates, L.A., Aandahl, Z., Richards, S.A., Brook, B.W., 2023. Cross validation for model selection: a review with examples from ecology. Ecol. Monograph. 93 (1), e1557.

Zischg, A., Huber, B., Frehner, M., Könz, G., 2021. Berechnung der Vegetationshöhenstufen auf der Grundlage der CH2018 Szenarien für die Schweiz. Schlussbericht, Abenis AG; Geographisches Institut der Universität Bern, Chur; Bern.

Zollner, P.A., Gustafson, E.J., He, H.S., Radeloff, V.C., Mladenoff, D.J., 2005. Modeling the influence of dynamic zoning of forest harvesting on ecological succession in a northern hardwoods landscape. Environ. Manag. 35 (4), 410–425.

Further reading

Abegg, M., Ahles, P., Allgaier Leuch, B., Cioldi, F., Didion, M., Düggelin, C., Fischer, C., Herold, A., Meile, R., Rohner, B., Rösler, E., Speich, S., Temperli, C., Traub, B., 2023a. Swiss National Forest Inventory - Result table No. 1331473. http://dx.doi.org/10.21258/1868871, Swiss Federal Research Institute WSL, Place: Birmensdorf, URL: https://doi.org/10.21258/1868871, Accessed: 2025-08-14.

Abegg, M., Ahles, P., Allgaier Leuch, B., Cioldi, F., Didion, M., Düggelin, C., Fischer, C., Herold, A., Meile, R., Rohner, B., Rösler, E., Speich, S., Temperli, C., Traub, B., 2023b. Swiss National Forest Inventory - Result table No. 1346822. http://dx.doi.org/10.21258/1895322, Swiss Federal Research Institute WSL, Place: Birmensdorf, URL: https://doi.org/10.21258/1895322, Accessed: 2025-08-14.

Akiba, T., Sano, S., Yanase, T., Ohta, T., Koyama, M., 2019. Optuna: A Next-generation hyperparameter optimization framework. In: Proceedings of the 25th ACM SIGKDD International Conference on Knowledge Discovery and Data Mining.

Allgaier Leuch, B., Streit, K., Stillhard, J., Cioldi, F., Brang, P., 2018. Zukunft der Fichte im Schweizer Mittelland. Wald. Und Holz (3), 31–34.

Bugmann, H., Brang, P., Elkin, C., Henne, P., Jakoby, O., Lévesque, M., Lischke, H., Psomas, A., Rigling, A., Wermelinger, B., Zimmermann, N., 2014. Climate Change Impacts on Tree Species, Forest Properties, and Ecosystem Services. pp. 79–90.

Didion, M., Kaufmann, E., Thürig, E., 2014. Estimating Carbon Stock Changes in Living and Dead Biomass and Soil for Switzerland's Forest management reference level – Modeling Methodology and Results. Technical Report, Swiss Federal Institute for Forest, Snow and Landscape Research WSL, Birmensdorf.

Frehner, M., Wasser, B., Schwitter, R., 2005. Nachhaltigkeit und erfolgskontrolle im schutzwald. Bern Wegleitung Für Pflegemassnahmen Wäldern Mit Schutzfunktion. Bundesamt Für Umw. Wald. Und Landsch. Bern 564.

Mina, M., Bugmann, H., Klopcic, M., Cailleret, M., 2017. Accurate modeling of harvesting is key for projecting future forest dynamics: a case study in the Slovenian mountains. Reg. Environ. Chang. 17 (1), 49–64. http://dx.doi.org/10.1007/s10113-015-0902-2.

Ploton, P., Mortier, F., Réjou-Méchain, M., Barbier, N., Picard, N., Rossi, V., Dormann, C., Cornu, G., Viennois, G., Bayol, N., et al., 2020. Spatial validation reveals poor predictive performance of large-scale ecological mapping models. Nat. Commun. 11 (1), 4540.

Rasche, L., Fahse, L., Zingg, A., Bugmann, H., 2011. Getting a virtual forester fit for the challenge of climatic change. J. Appl. Ecol. 48 (5), 1174–1186. http://dx.doi.org/10.1111/j.1365-2664.2011.02014.x, URL: https://besjournals.onlinelibrary.wiley.com/doi/abs/10.1111/j.1365-2664.2011.02014.x, _eprint: https://besjournals.onlinelibrary.wiley.com/doi/pdf/10.1111/j.1365-2664.2011.02014.x.

Shekhar, S., Bansode, A., Salim, A., 2022. A comparative study of hyper-parameter optimization tools. CoRR abs/2201.06433, arXiv:2201.06433, URL: https://arxiv.org/abs/2201.06433, arXiv:2201.06433.

Stadelmann, G., 2020. Quantifizierung der Waldbiomasse und des Holznutzungspotenzials in der Schweiz. Schweiz. Z. Für Forstwes. 171 (3), 124–132. http://dx.doi.org/10.3188/szf.2020.0124.

Thürig, E., Portier, J., Allgaier Leuch, B., Cioldi, F., Herold, A., Stadelmann, G., Temperli, C., Wohlgemuth, T., Rohner, B., 2025. Die Schweizer Holzressourcen im Wandel: Trends aus 40 Jahren LFI. In: Schweizerische Zeitschrift für Forstwesen, 176(5). pp. 244–253. http://dx.doi.org/10.3188/szf.2025.0244.

Valavi, R., Elith, J., Lahoz-Monfort, J.J., Guillera-Arroita, G., 2018. blockCV: An R package for generating spatially or environmentally separated folds for k-fold cross-validation of species distribution models. Biorxiv, 357798.

xgboost developers, 2022. XGBoost Parameters — xgboost 3.0.2 documentation. URL: https://xgboost.readthedocs.io/en/stable/parameter.html, URL: https://xgboost.readthedocs.io/en/stable/parameter.html, Accessed: 2025-07-09.